STUDIES ON MAGNETIC RECORDING

W. K. WESTMIJZE

Kast dissertaties

STUDIES ON MAGNETIC RECORDING

PROEFSCHRIFT

TER VERKRIJGING VAN DE GRAAD VAN DOCTOR IN DE WIS- EN NATUURKUNDE AAN DE RIJKSUNIVERSITEIT TE LEIDEN OP GEZAG VAN DE RECTOR MAGNIFICUS DR J. J. L. DUYVENDAK, HOOGLERAAR IN DE FACULTEIT DER LETTEREN EN WIJSBEGEERTE, TEGEN DE BEDENKINGEN VAN DE FACULTEIT DER WIS- EN NATUURKUNDE TE VERDEDIGEN OP WOENSDAG 25 MAART 1953 TE 15 UUR

DOOR

WILLEM KLAAS WESTMIJZE

GEBOREN TE ROTTERDAM IN 1918

PROMOTOR: PROF. DR H. B. G. CASIMIR

Aan de nagedachtenis van mijn Vader
Aan mijn Moeder
Aan Ivette

VOORWOORD

Onder de verschillende methoden die tegenwoordig worden gebruikt om geluid te registreren neemt de magnetische registratie een steeds belangrijker plaats in. Hoewel men de problemen die erbij optreden als electrotechnische problemen zou kunnen betitelen blijkt het toch dat bij de studie van dit procédé van geluidsweergave een aantal onderwerpen ter sprake komen, die op zichzelf belangwekkend zijn terwijl omgekeerd deze technische problemen een fraai voorbeeld zijn van toepassing der methoden der mathematische physica. Enkele problemen kunnen slechts tot oplossing worden gebracht door gebruik te maken van de moderne inzichten in het ferromagnetisme, terwijl anderzijds bepaalde verschijnselen die ook theoretisch van belang zijn, bijv. de magnetische nawerking, op deze manier goed kunnen worden bestudeerd.

In dit proefschrift zullen hoofdzakelijk deze principiele vraagstukken besproken worden en op technische toepassingen zal alleen worden ingegaan voor zover dit voor de principiele problemen van belang is.

Het is mij een behoefte op deze plaats mijn hartelijke dank te betuigen aan de Directie van het Natuurkundig Laboratorium der N.V. Philips' Gloeilampenfabrieken voor de gelegenheid die ze mij gegeven heeft om aan dit proefschrift te werken en voor de daarbij ondervonden steun.

Ook aan vele medewerkers van het laboratorium ben ik dank verschuldigd voor de ondervonden samenwerking. In het bijzonder geldt deze dank Ir. R. Vermeulen voor zijn stimulerende leiding en Ir. D. Kleis voor de vele uitvoerige discussies die we mochten hebben.

CONTENTS

Part VI. **Change in the recording with time**

I. INTRODUCTION

1. Description of the method of magnetic recording

In magnetic recording a magnetizable medium is moved at constant speed along a magnetic structure (recording head) which is capable of inducing in the medium a magnetization proportional to the current fed to the structure. In this way the variation of the current with time is recorded in the tape as a variation of the magnetization with distance.

This varying magnetization produces a magnetic field around the medium which, if the medium is brought near a reproducing head, gives rise to a flux through the pick-up coil of the head, proportional to the magnetization in the tape. During play-back the medium is moved with the same speed as during recording past this reproducing head where the flux variations induce a voltage over the coil.

In the case of tape recording, to which we will restrict ourselves, the arrangement may be as shown in fig. 1. The tape B, pressed by a roller R against a capstan A, is forced in the indicated direction. On its way the tape passes three heads K_1, K_2 and K_3. The first is an erasing head which obliterates anything which may have previously been recorded on the tape and makes the tape susceptible to the registration of new magnetization by the recording head K_2. The reproducing head K_3 may read the magnetization in the tape recorded a moment before by K_2 or, if K_1 and K_2 are out of action, the magnetization that has been recorded earlier on the tape stored on the reel M_1.

The tape speed depends on the purpose for which the recording has to be used. For professional use where the quality of the recording is of primary importance, the standardized speeds are 762 or 381 mm/sec (30

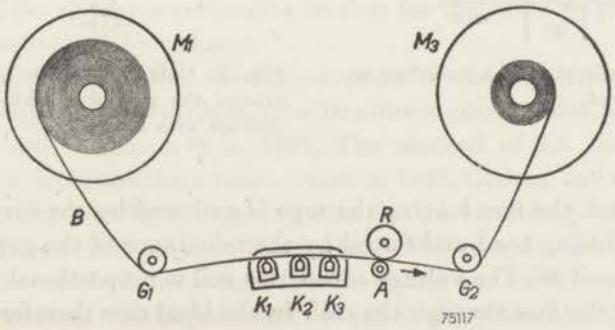

Fig. 1. Schematic arrangement of a magnetic recorder.

or 15 in/sec) allowing the reproduction of a frequency range from 30 to 15000 Hz. For popular recording the economy of tape use is important and consequently the speed is lower, but even with a speed of 95 mm/sec ($3\frac{3}{4}$ in/sec) a reproduction of frequencies up to 5000 Hz is possible. In this case separate recording and reproducing heads are seldom found, a single head being alternately used for recording and reproduction.

The tape may be of two types; either a magnetic powder is worked homogeneously through a nonmagnetic carrier, or a thin coating of magnetic powder in a binding material covers a nonmagnetic carrier (inhomogeneous or coated tapes). In both cases the total thickness of the tape is about 55 μm. The magnetic powder used is mostly γFe_2O_3 or Fe_3O_4, the particle size averaging less than one micron.

Since the time of Schüller[1]) the heads, erasing and recording, as well as reproducing, are generally of the ring-shaped type (fig. 2). Here the tape passes in front of the gap S in a, usually lamellated, highly-permeable core structure K. In erasing and recording the tape traverses the stray field around the gap S caused by a current through the coil W. The erasing field has a frequency well above the highest to be recorded, and an amplitude that can effect saturation of the tape. In order to obtain a linear relationship between the signal current and the recorded magnetization an alternating current having an equally high or even higher frequency is superimposed on the signal current.

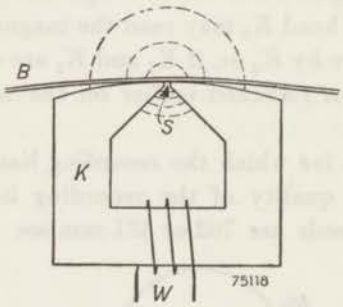

Fig. 2. Schematic view of a recording or reproducing head.

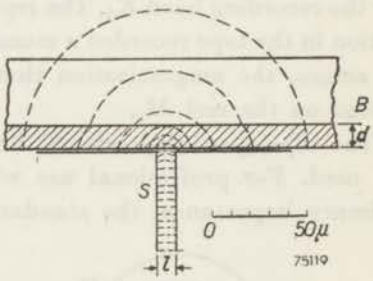

Fig. 3. Enlarged sketch of the region around the gap of a magnetic head in contact with a tape.

In play-back the flux leaving the tape is gathered by the core structure of the reproducing head and forced by the reluctance of the gap to thread through the coil W. The voltage across this coil is proportional to the rate of change of the flux through the coil. In the ideal case therefore this voltages rises proportionally with the frequency.

In order to illustrate the relative proportions fig. 3 gives an enlarged sketch of the region of the gap in contact with the tape for a practical recording or reproducing head. A more elaborate review of the technical side of magnetic recording is given by Begun [2]).

2. Historic survey

Although it is only in recent years that magnetic recording has started to come into general use, its invention by the Danish engineer Valdemar Poulsen [3]) dates back as far as 1898. He constructed an apparatus in which a steel wire wound on a cylinder was moved between two pole-pieces of a head which acted for recording as well as for reproducing. In this way he was able to register the current from a microphone, and in reproduction to make the registration audible with an earphone. This apparatus, the telegraphone, was demonstrated at the Paris exposition in 1900.

In itself, the reproduction of sound was known already, since it was in 1877 that Edison demonstrated his phonograph. It was, however, only at the time of Poulsen's invention that the first commercial records were made.

In disc recording the energy obtained from the disc is sufficient to effect a reasonable sound level in a room. The magnetic registration on the contrary, without amplification could only be heard with earphones, and it is due to this fact that interest in magnetic recording died down until about 1925. Then, with the possibility of electronic amplification, research was resumed. That quite a lot of progress had to be made is illustrated by the fact that for reproduction of frequencies up to 5000 Hz the steel tape in the machine used by Stille [4]) in 1930 had to run at a speed of 2 m/sec., that is about 20 times greater than is required nowadays.

The reason for the difference lies for an important part in the kind of tape used, viz. the steel tape with a high permeability and low coercivity. An enormous step forward therefore was the development of the powder-coated tape, based on the invention of Pfleumer [5]). This type of tape, combined with the ring-head of Schüller mentioned above, enabled the recording of far shorter wavelengths so that for the same frequency range the tape speed could be reduced.

A last decisive step was the introduction of the high-frequency bias. Until then linearization was obtained with a direct-current bias, as indicated by Poulsen and Pederson [6]) in 1907. The method of a.c. biasing seems to have been invented three times. First, in 1922, Carlson and Carpenter [7]) used a superimposed high-frequency bias for the recording on steel wire. The method, however, got into disuse. In 1938 Nagai, Sasaki and Endo [8]) described the method, this time for recording on steel tape, drawing special attention to the improvement it effected by diminishing the noise and extending the linear part of the recording characteristic. It was not,

however, until 1941 that v. Braunmühl and Weber [9]) introduced the method in combination with the improved heads and tape, thus bringing the quality of the magnetic recording up to the standard of any other sound-recording system.

3. Outline of present work

If the practice of magnetic recording has reached a state of perfection this is not because it could be based on a solid theoretical foundation. In the rapidly expanding literature on the subject the number of theoretical contributions is remarkably small.

This is mainly due to the circumstance that the subject is on the one hand rather complicated but on the other hand of too technical a nature to attract the attention of physicists interested in the more fundamental aspects of magnetism.

During recording the tape traverses a magnetic field that is inhomogeneous and varying with time, the time variations, moreover, consisting of a superposition of the low frequency to be recorded on of the high frequency of the biasing field. The particles subjected to this field differ amongst each other in size and magnetic properties. For the particles at different depth in the tape the amplitude of the field variations is different, resulting in a recorded magnetization that varies with the depth in the tape. Once the signal is recorded, an interaction occurs between places in the tape with different magnetization, giving rise to a demagnetizing field and a decrease of the recorded magnetization. The best way to study what is recorded on the tape is to bring it into contact with a reproducing head, but in doing so the demagnetizing field is affected. Further complications are due to the non-ideal contact between tape and head (to which the output is very sensitive), to the finite thickness of the tape, and to the finite length of the reproducing gap.

A consequence of this intricacy is that it is seldom possible to determine by direct measurement the influence of one or another of the factors summed up separately above. For a theoretical discussion simplifying assumptions have to be made; and because of the difficulty of following the processes step-by-step, it is mostly impossible directly to control the error caused by these simplifications.

It is not the aim of the present work to go into all the details of the magnetic recording method. Only some subjects will be selected from those that have a direct physical or mathematical background. Although the insight obtained in this way may lead to practical conclusions these will not be discussed at length.

Starting from a given current through the coil of the recording head we shall calculate in Part II the magnetic stray-field in front of the gap of

different types of head. One type resembles in its essentials the existing heads. The two others are only theoretical cases, but they form more or less extremes on both sides of the actual head.

Once the field distribution in front of the head is known, the sequence of magnetic fields that an element of tape traverses in passing the head is also known and it should be possible to determine the ultimate magnetization of this element. We will confine ourselves to the quasi-stationary case, which means that the element is subjected to a great number of cycles of the biasing field and that therefore the difference between two succeeding loops is very small; there is then close resemblance to the method of ideal magnetization. The discussion of this case in Part III will be based on measurements in homogeneous fields. These measurements show how the superposition of an h.f. field of sufficient strength on the direct field results in a linear relation between the direct field and the recorded magnetization. The physical background of this linearizing action is discussed.

If instead of a direct current an alternating current of low frequency is recorded, the recorded magnetization usually appears to decrease with increasing frequency. This is sometimes called frequency distortion or linear distortion, for it means that though at every frequency the recorded magnetization is proportional to the magnetizing low-frequency field, the proportionality constant depends on the frequency.

The losses in the output at the higher frequencies may be divided into two categories, viz. those losses which depend on frequency only (caused for instance by the eddy currents in the recording head), and those which depend on the recorded wavelength only. Experimentally the frequency-dependent and the wavelength-dependent losses may be separated by making measurements at different tape speeds. In the following pages we will only occupy ourselves with the latter category. These losses may occur at different stages in the chain: recording head-tape-reproducing head and it is difficult to determine how the overall losses are divided over the different sources; these sources are:

(1) During the time the tape passes the finite length in front of the recording gap where the magnetization process takes place, the phase of the high signal-frequency to be recorded changes, thus effecting a weakening of the recorded magnetization. This phase change is proportional to the frequency f and inversely proportional to the tape speed v, so this recording loss depends on the wavelength $\lambda = v/f$.
(2) Demagnetization in the tape after the recording process has taken place.
(3) Finite thickness of the tape and space between tape and reproducing head.

(4) Finite length*) of the reproducing gap.

In his excellent treatise Lübeck [10]) ascribes most of the observed difference between the theoretical and the observed response curve to the demagnetization. Herr, Murphy and Wetzel [11]), however, point out the important influence of tape thickness and distance between tape and head on the response curve, which is confirmed by the calculation of Wallace [12]) for a tape of unit permeability.

In part IV we shall calculate the influence of demagnetization on the response curve for a tape with a permeability greater than unity. The boundary problem is solved for a tape of infinite width and a prescribed initial magnetization, bounded on one side at a certain distance by the highly permeable metal of the head. The solution gives the fields in and around the tape, and enables us to calculate the flux entering the head for the case of the gap being infinitely short. As will be seen the thickness of the tape and the separation between head and tape both have an influence on the reproduced flux. It is, however, not possible to separate the influence of the one from that of the other, since the presence of the reproducing head affects the demagnetizing field to a degree that depends on distance.

For the case where the reproducing gap has a finite length it is no longer possible to give a simple solution of the potential problem. We are interested in the ability of the head to pick up the flux from the tape when the recorded wavelength is comparable with the gap length. Applying the reciprocity theorem we can calculate this flux for a given magnetization of the tape if the field configuration round an energized head is known. Since this field configuration is calculated in Part II we shall in that part also calculate the gap loss.

With the calculations and measurements of Parts II to IV it is in principle possible to calculate the magnetization recorded in a tape and the flux through a reproducing head as a consequence of this magnetization. In part V we shall compare the calculated magnetization with measurements. By a suitable choice of biasing- and signal-current the distortion can be kept below a level sufficiently low even for sound recording, while the frequency characteristic is such that sound can be recorded up to the highest audible frequency without too high speeds of the tape. Moreover, to attain a flat frequency response, correcting networks can be used.

This correction is limited by the background noise which, for sound recording, has to be kept at a very low level. We shall not enter in detail

*) It is convenient to use for the head the same indications of direction as for the tape. Hence the length of the gap means the dimension in the direction of movement of the tape (l in fig. 3).

into the nature of the background noise, but we only mention that a certain amount of noise is to be expected from the nature of the recording material. This consists of very fine magnetic particles distributed throughout the binding material. These particles are built up of one or more Weiss domains which are always magnetically saturated. Their stray fields will therefore impart a flux to the reproducing head during their passage past the gap. The random distribution of these particles causes a noise, even if the tape as a whole is demagnetized, owing to the random distribution of the directions of magnetization.

A question of considerable interest is what happens to a tape once a magnetization is recorded. Two things are of importance here. Firstly, does the magnetization decrease in the long run, especially if exposed to the demagnetizing fields that exist if the recorded wavelength is small? Secondly, what happens if the tape is exposed to small fields, especially those originating in the magnetization of an adjacent winding if a tape is stored on a reel? This question will be treated in Part VI, where measurements are given and explained as a diffusion process caused by the Brownian motion.

Throughout this work the Giorgi unit-system is used. Therefore the magnetic induction B, like the magnetization M, is expressed in Vsec/m^2 and the field strength in A/m.

In order to make comparison with the Oersted more easy we shall for numerical data give $\mu_0 H$ in Vsec/m^2 ($\mu_0 = 4\pi \cdot 10^{-7}$ Vsec/Am), so that the field strength in Oersted is obtained by multiplying these data with 10^4.

We shall confine the use of the symbol μ to the relative permeability; thus the relation between induction and field strength for isotropic linear media is given by $\boldsymbol{B} = \mu\mu_0\boldsymbol{H}$ and the magnetization $\boldsymbol{M}$ by $\boldsymbol{M} = \boldsymbol{B} - \mu_0\boldsymbol{H}$.

To avoid the possibility of confusion between permeability and micron in the sense of 10^{-6} m, we shall denote the latter by μm. This procedure is indeed proposed in the International Standard Organization.

For reasons of standardization the symbol Hz is preferred to that of c/s for the indication of the number of periods per second,

II. FIELD CONFIGURATION AROUND THE GAP AND THE GAP-LENGTH FORMULA

1. Types of head to be discussed

We are interested in the configuration of the magnetic field around the gap for two reasons; (1) on the recording side it informs us about the magnetic fieldstrengths the tape traverses in passing the gap, while (2) on the reproducing side it enables us, making use of the reciprocity theorem, to calculate the flux through the coil of the reproducing head due to the presence of a sinusoidally magnetized tape. This may be shown as follows.

The field distribution being known, the flux Φ through an arbitrary cross-section of the tape caused by a current I through the coil is also known. Now the reciprocity theorem states that, on the other hand, a current I round this cross-section of the tape excites the same flux Φ through the coil of the head. Replacing the tape by a series of currents of appropriate strength round the tape, the resulting flux through the coil of the head may be found by summing the contributions of all these currents.

It is easily seen that if the recorded wavelength is long compared with the length of the gap and small compared with the length of the head, the flux through the coil equals the flux in the tape in front of the gap. Deviations occur, if the wavelength is of the order of the length of the head or of the order of the gap length.

We are chiefly interested in the latter case. Here the contributions to the flux are mainly due to elements of the tape in the neighbourhood of the gap. So it makes no difference if we suppose the head to be infinitely extended in the longitudinal direction of the tape.

A further simplifying assumption, which makes the potential problem a two-dimensional one, is that both the tape and the head are of infinite width. Finally we suppose the permeability of the tape to be unity, and that of the head to be infinite.

We shall discuss in this section three types of head (fig. 4). In the first one (fig. 4*a*) the gap is formed by two parallel planes $x = -l/2$ and $x = +l/2$. The tape is moved parallel to the x-axis. Although this type of head is impracticable, for the tape would have to cross an infinitely small slit in the walls of the gap, it is of some theoretical interest. The fieldstrength in this gap is easily calculated, and it is for this simple model that the well-known gap-loss formula $\{\sin(\pi l/\lambda\}/(\pi l/\lambda)$ holds.

The second type (fig. 4*b*) is formed by two thin sheets, extending in the

plane $y = 0$, one from $x = -\infty$ to $x = -l/2$, and the other from $x = l2$ to $x = \infty$. This model resembles more or less some heads used in practice. The field distribution as well as the gap-length formula can be calculated.

In the third type (fig. 4*c*) the left pole piece is bounded by the plane $y = 0$ from $x = -\infty$ to $x = -l/2$ and by the plane $x = -l/2$ from $y = 0$ to $y = -\infty$. The right pole piece is symmetrical to the left with respect to the plane $x = 0$. This type bears close resemblance to practical heads, but the calculations are rather difficult to carry out.

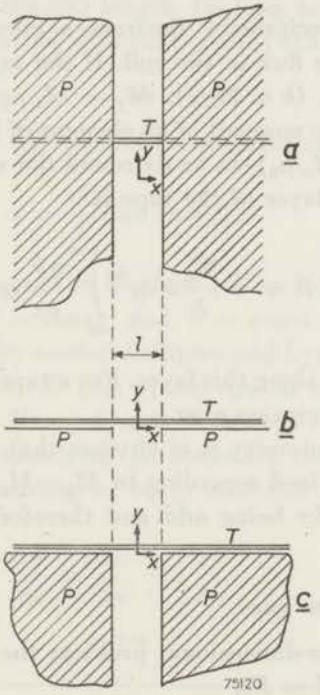

Fig. 4. Shape of the pole pieces P and relative position of an element of tape T for the three types of head discussed.
a. Infinite gap: *b*. "Thin" gap; *c*. Semi-infinite gap.

Seen in the direction normal to the tape the gap is infinitely extended in both the positive and the negative direction in the first type, in the second it is infinitely small, while in the third type it is infinitely extended only in the negative direction. Thus the latter type is intermediate between the other two.

In all three cases the permeability of the head material is supposed to be infinite, so that the pole surfaces are magnetic equipotentials. The coil of the head, consisting of one turn, may be supposed to be wound round

a connecting element of the two pole-pieces. A current I through this coil results in a magnetic potential difference I between the pole pieces. Thus the potential function $V(x, y)$ solving the problem has to satisfy the boundary condition $V = \frac{1}{2} I$ and $= -\frac{1}{2} I$ respectively for the two pole-pieces. From the symmetry it is clear that $V = 0$ for $x = 0$.

A current I through the head excites in an element of the tape of width b and thickness dy a flux

$$d\Phi = -\mu_0 \frac{\partial V}{\partial x} b \, dy .$$

According to the reciprocity theorem a current I round the element $b dy$ excites the same flux in the coil. If the tape is magnetized according to $M_x = M_0 \cos kx$, $(k = 2\pi/\lambda)$, $M_y = M_z = 0$ (longitudinal magnetization), the magnetic moment of an element of length dx will be equivalent to a current $I' = (M_0/\mu_0) \cos kx \, dx$ round the element. So the flux in the coil caused by this layer of the tape is

$$d\Phi = -\frac{M_0}{I} b \, dy \int_{-\infty}^{+\infty} \frac{\partial V}{\partial x} \cos kx \, dx . \qquad (1)$$

Here $\partial V/\partial x$ is taken along this layer. For a tape of finite thickness the total flux is found by integration over y.

For reasons of symmetry it is obvious that $\partial V/\partial x$ is an even function. Thus a tape magnetized according to $M_x = M_0 \sin kx$ will induce no flux in the coil, $\partial V/\partial x \sin kx$ being odd and therefore integration from $-\infty$ to $+\infty$ giving zero.

2. **First type, infinite gap**

In this simple one-dimensional problem the potential is $V = Ix/l$, and the fieldstrength $H = I/l$.

The flux coming from a cross section $b dy$ of a tape magnetized according to $M_x = M_0 \cos kx$ is (eq. 1)

$$d\Phi = -\frac{M_0}{I} b \, dy \int_{-l/2}^{+l/2} \frac{I}{l} \cos kx \, dx = M_0 \, b \, dy \, \frac{\sin(kl/2)}{kl/2} .$$

The contribution of a tape of thickness d and width b is

$$\Phi = M_0 \, bd \, \frac{\sin(kl/2)}{kl/2} = \Phi' \, G(\pi l/\lambda) , \qquad (2)$$

where $\Phi' = M_0 \, bd$ and $G(x) = \sin x/x$.

This is the well-known gap-loss formula, derived by Lübeck [10]) for a head of type *c*. The assumption Lübeck makes in the derivation is that the lines of force leaving the tape are distributed in inverse proportion to the distance to the pole pieces. This condition is fulfilled in the case discussed here, but not, as we shall see, for a head of type *b* or *c*.

This gap-loss formula bears close resemblance to the formula for the loss due to the finite width of the light-slit in optical recording and reproduction. In the latter case, however, the amplitude is proportional to the width of the light-slit, while in the case discussed here for long wavelengths the flux is independent of the gap length, (as long as the reluctance of the air gap remains great compared with that of the path through the coil).

3. Second type, "thin" gap

In order to discuss case *b* we consider the transformation

$$z = \frac{il}{2} \sinh (\pi W/I) \tag{3}$$

giving a conformal mapping of the W-plane ($W = U + iV$) on the z-plane ($z = x + iy$). The lines $U =$ const. and $V =$ const. in the W-plane are represented in the z-plane by confocal ellipses and hyperbolas recpectively. The line segments AB and CD (fig. 5) are special cases of the confocal hyperbolas, attained for $V = \frac{1}{2} I$ and $V = -\frac{1}{2} I$ respectively. So the potential function $V(x, y)$ satisfying the boundary conditions of our problem may be found by separating in eq(3) real and imaginary parts and eliminating U.

Since
$$\frac{dW}{dz} = \frac{\partial U}{\partial x} + i \frac{\partial V}{\partial x},$$

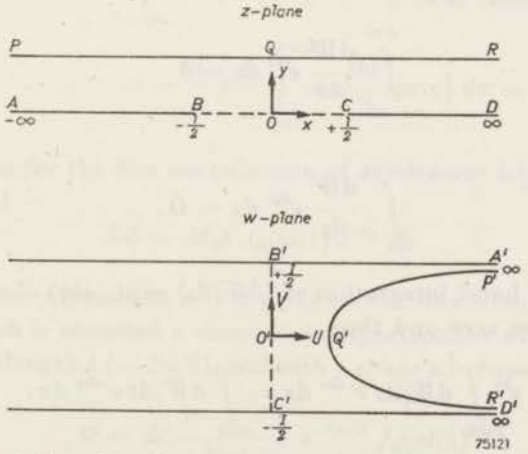

Fig. 5. Mapping of the z-plane ($z = x + iy$) on the W-plane ($W = U + iV$) for case *b*.

or, with the Cauchy-Riemann relation $\partial U/\partial x = \partial V/\partial y$,

$$\left|\frac{dW}{dz}\right| = \frac{\partial V}{\partial y} + i\frac{\partial V}{\partial x},$$

it follows that the absolute value of the fieldstrength is given by

$$\sqrt{\left(\frac{\partial V}{\partial x}\right)^2 + \left(\frac{\partial V}{\partial y}\right)^2} = \left|\frac{dW}{dz}\right|.$$

Thus in our case the fieldstrength $H_n = -\partial V/\partial z$ normal to the planes $V =$ constant is found by taking the absolute value of

$$\frac{dW}{dz} = -i\frac{2}{\pi}\frac{I}{l}\{1-(2z/l)^2\}^{-1/2},$$

therefore

$$H_n = \frac{2}{\pi}\frac{I}{l}\left|\{1-(2z/l)^2\}^{-1/2}\right|.$$

For the special case $x = 0$ we have

$$H_x = \frac{2}{\pi}\frac{I}{l}\{1+(2y/d)^2\}^{-1/2}.$$

To obtain the flux induced in the coil of the reproducing head by a magnetized tape in a plane $y =$ constant $\int_{-\infty}^{+\infty} \partial V/\partial x \cos kx\, dx$ has to be calculated, where $\partial V/\partial x$ is taken along the line PQR in the z-plane.

Since for $z \to \infty$, $|dW/dz| \to 0$ integration of $(dW/dz)\exp(ikz)$ along the semicircles in infinity in the upper half of the z-plane gives zero. Thus for any line $y =$ const. $\geqslant 0$

$$\int_{x=-\infty}^{+\infty} \frac{dW}{dz} e^{ikz}\, dz = 0$$

and therefore

$$\int_{-\infty}^{+\infty} \frac{dW}{dz} e^{ikx}\, dx = O. \tag{4}$$

On the other hand integration of $(dW/dz)\exp(-ikz)$ along the contour $AODRQPA$ gives zero and thus

$$e^{ky}\int_{PQR} dW/dz\, e^{-ikx}\, dx = \int_{AOD} dW/dz\, e^{-ikx}\, dx. \tag{5}$$

Therefore with eq. (4)

$$e^{ky} \int_{PQR} \frac{dW}{dz} \cos kx \, dx = \int_{AOD} \frac{dW}{dz} \cos kx \, dx$$

or

$$\int_{PQR} \left(\frac{\partial U}{\partial x} + i \frac{\partial V}{\partial x} \right) \cos kx \, dx = e^{-ky} \int_{AOD} \left(\frac{\partial U}{\partial x} + i \frac{\partial V}{\partial x} \right) \cos kx \, dx .$$

Taking the imaginary part on both sides it follows that

$$\int_{PQR} \frac{\partial V}{\partial x} \cos kx \, dx = e^{-ky} \int_{AOD} \frac{\partial V}{\partial x} \cos kx \, dx . \tag{6}$$

This is a general formula that holds provided only that $|dW/dz| \to 0$ for large values of $|z|$. Since in our case $\partial V/\partial x = 0$ along AB and CD the integration on the right hand side can be taken over BOC.

To evaluate the integral on the right hand side of eq. (6) we have to find the dependence of $x(V)$ on V for the x-axis.

From eq. (3) it follows by separating the real and imaginary parts

$$x = -\frac{l}{2} \cosh \frac{\pi U}{I} \sin \frac{\pi V}{I}$$

$$y = \frac{l}{2} \sinh \frac{\pi U}{I} \cos \frac{\pi V}{I} .$$

Thus for $y = 0$ it follows that $U = 0$, and therefore $x = -(l/2) \sin (\pi V/I)$. Eq. (6) now becomes

$$\int_{PQR} \frac{\partial V}{\partial x} \cos kx \, dx = e^{-ky} \int_{+I/2}^{-I/2} \cos \left\{ k \left(-\frac{l}{2} \sin \frac{\pi V}{I} \right) \right\} dV =$$

$$= -\frac{I}{\pi} e^{-ky} \int_{-\pi/2}^{+\pi/2} \cos \left(\frac{kl}{2} \sin \tau \right) d\tau = -I \, e^{-ky} J_0 \left(\frac{kl}{2} \right) .$$

So we obtain for the flux contribution of an element $b dy$ at a distance y from the head

$$d\Phi = M_0 b \, J_0(kl/2) \, e^{-ky} \, dy .$$

Integration over y from a to $a + d$ gives for the flux from a tape of thickness d on which is recorded a sinusoidal magnetization with an amplitude M_0 and a wavelength λ $(= 2\pi/k)$, and with a space a between head and tape

$$\Phi = \Phi' \frac{1 - e^{-2\pi d/\lambda}}{2\pi d/\lambda} e^{-2\pi a/\lambda} J_0(\pi l/\lambda) \tag{7}$$

where $\Phi' = M_0 bd$.

From a tape magnetized according to $\Phi' \cos \{2\pi(x-x')/\lambda\}$ only the even term $\Phi' \cos(2\pi x/\lambda) \cos(2\pi x'/\lambda)$ contributes to the flux in the coil. If the tape is moved with a speed v along the head ($x' = vt$) the flux in the head is

$$\Phi' \frac{1-e^{-2\pi d/\lambda}}{2\pi d/\lambda} e^{-2\pi a/\lambda} J_0(\pi l/\lambda) \cos \omega t; \quad (\omega = 2\pi v/\lambda)$$

and hence eq. (7) represents the amplitude of the flux variation in the head if a sinusoidally magnetized tape is moved along the head.

The three factors describing the influence of tape thickness d, space between head and tape a, and gap length l are occurring separately. Thus the gap loss is given by the Bessel function $J_0(\pi l/\lambda)$, independent of tape thickness and distance head to tape. In fig. 9 this function is plotted against l/λ. Comparison with the gap-loss function $\{\sin(\pi l/\lambda)\}/(\pi l/\lambda)$ for a head of type a shows that the decrease of the amplitude of the maxima and minima is slower. This is also shown by the first term of the asymptotic expansion of the Bessel function

$$J_0(\pi l/\lambda) \approx \frac{\sin(\pi l/\lambda + \pi/4)}{\pi\sqrt{l/2\lambda}}.$$

The above solution of the potential problem also holds if, instead of the boundary discussed, the pole pieces are bounded by two blades of hyperbolas with focal points B and C (fig. 5). However, a tape parallel to the x-axis is impossible in this case for it has to cross the pole pieces. When, however, this cross point occurs for x large as compared with the gap-length it makes a negligible difference on the flux in the coil if for larger x the tape follows the surface of the head instead of crossing it.

4. Third type, semi infinite gap

In this case the potential problem can be solved with the Christoffel-Schwarz-method. Because of the symmetry it is sufficient to consider the problem where the potential of ABC (fig. 6) is $\frac{1}{2}I$, and that of DE is zero. Application of the theorem of Schwarz and Christoffel gives as the equation from which the transformation of the contour $ABCDE$ in the z-plane into the ξ-axis of the ζ-plane ($\zeta = \xi + i\eta$) is found

$$\frac{dz}{d\zeta} = C \frac{\sqrt{\zeta}}{\zeta - 1},$$

which integrates to

$$z = 2C\left(\sqrt{\zeta} + \tfrac{1}{2} \ln \frac{\sqrt{\zeta}-1}{\sqrt{\zeta}+1}\right) + C'.$$

If $\sqrt{\zeta}$ is defined such that $\sqrt{\zeta}$ lies in the first quadrant for $\mathrm{Im}(\zeta) > 0$, and

the logarithm such that for $\zeta \to \infty$, $\ln\{(\sqrt{\zeta}-1)/(\sqrt{\zeta}+1)\} \to 0$ the values of the constants C and C' are found to be $C = il/2\pi$ and $C' = 0$. The required transformation now becomes

$$x = \frac{il}{\pi}\left(\sqrt{\zeta} + \tfrac{1}{2}\ln\frac{\sqrt{\zeta}-1}{\sqrt{\zeta}+1}\right). \tag{8}$$

On the other hand the equation

$$W = \frac{I}{2\pi}\ln(\zeta - 1);\ (W = U + iV) \tag{9}$$

transforms the W-plane into the ζ-plane such that, if the logarithm is real for $\zeta > 1$, $V = 0$ is mapped on $D'E'$, and $V = \frac{1}{2}I$ on $A'C'$. In general a line $V = V_0$ in the W-plane is mapped in the ζ-plane on a straight line through the point $C'(1, 0)$ making an angle $2\pi V_0/I$ with the positive ξ-axis.

Elimination of ξ from (8) and (9) gives the desired transformation, where V satisfies the potential equation and the boundary condition.

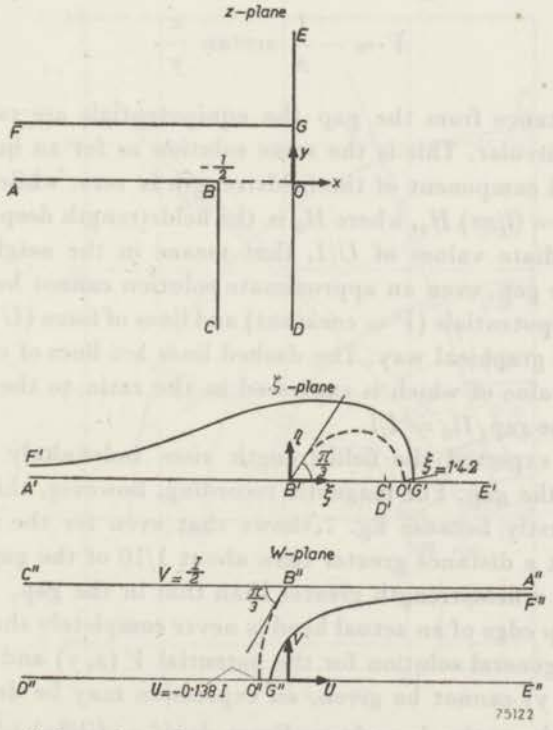

Fig. 6. Mapping of the z-plane ($z = x + iy$) and the W-plane ($W = U + iV$) on the ζ-plane ($\zeta = \xi + i\eta$) for case c.

An analogous solution has been given recently by Booth [13]).

It is impossible to give $V(x, y)$ in explicite form for the general case; this is only possible in the limiting cases $U/I \ll -1$ and $U/I \gg 1$.

For $U/I \ll -1$: $\quad |\zeta - 1| = |e^{2\pi W/I}| \ll 1$,

$$z \approx \frac{il}{\pi}(1 - \ln 2 + \pi W/I),$$

so that

$$V \approx -\frac{I}{l}x.$$

Because $y \approx lU/I$, and $U/I \ll -1$ this gives the solution deep into the gap. Here the equipotentials are straight lines parallel to the gap wall. The fieldstrength $H = I/l$.

For $U/I \gg 1$: $\quad \zeta \approx e^{2\pi W/I}, \quad z \approx \frac{il}{\pi}\sqrt{\zeta},$

thence

$$x + iy \approx i\frac{l}{\pi}e^{\pi U/I}\{\cos(\pi V/I) + i \sin(\pi V/I)\},$$

$$V \approx -\frac{I}{\pi}\arctan\frac{x}{y}.$$

At great distance from the gap the equipotentials are radial and the lines of force circular. This is the same solution as for an infinitely short gap. The radial component of the fieldstrength is zero, while the tangential $H_t = I/\pi r = (l/\pi r)\,H_0$, where H_0 is the fieldstrength deep into the gap.

For intermediate values of U/I, that means in the neighbourhood of the edge of the gap, even an approximate solution cannot be given. Fig.7 gives some equipotentials (V = constant) and lines of force (U = constant), calculated in a graphical way. The dashed lines are lines of constant fieldstrength, the value of which is expressed in the ratio to the fieldstrength H_0 deep into the gap, $H_0 = I/l$.

As may be expected the fieldstrength rises indefinitely towards the sharp edge of the gap. For magnetic recording, however, this has no real significance, firstly because fig. 7 shows that even for the sharp edge a tape passing at a distance greater than about 1/10 of the gap length does not experience a fieldstrength greater than that in the gap, and secondly because the gap edge of an actual head is never completely sharp.

Although a general solution for the potential $V(x, y)$ and for the fieldstrength $H(x, y)$ cannot be given, an expression may be derived for the fieldstrength along the boundary. From $\mathrm{d}z/\mathrm{d}\zeta = (il/2\pi)\sqrt{\zeta}/(\zeta - 1)$ and $\mathrm{d}W/\mathrm{d}\zeta = (I/2\pi)/(\zeta - 1)$ it follows that

$$\frac{dW}{dz} = -i\frac{I}{l}\frac{1}{\sqrt{\zeta}} = -i\frac{H_0}{\sqrt{\zeta}}. \tag{10}$$

Since

$$H = \sqrt{\left(\frac{\partial V}{\partial x}\right)^2 + \left(\frac{\partial V}{\partial y}\right)^2} = \left|\frac{dW}{dz}\right| = \frac{H_0}{|\sqrt{\zeta}|},$$

the transformation (8), representing z as a function of $\sqrt{\zeta}$, provides a relation between z and H in the case where $\sqrt{\zeta}$ can be expressed in $|\sqrt{\zeta}|$. This is true for the boundary lines, where ζ is real.

Thus for the segment AB, where $\zeta < 0$, we have $\sqrt{\zeta} = i\,|\sqrt{\zeta}| = iH_0/H$. Therefore

$$z = \frac{il}{\pi}\left(i\frac{H_0}{H} + \tfrac{1}{2}\ln\frac{iH_0 - H}{iH_0 + H}\right)$$

whence

$$x = -\frac{l}{\pi}\left(\frac{H_0}{H} + \arctan\frac{H}{H_0}\right),$$

$$y = 0.$$

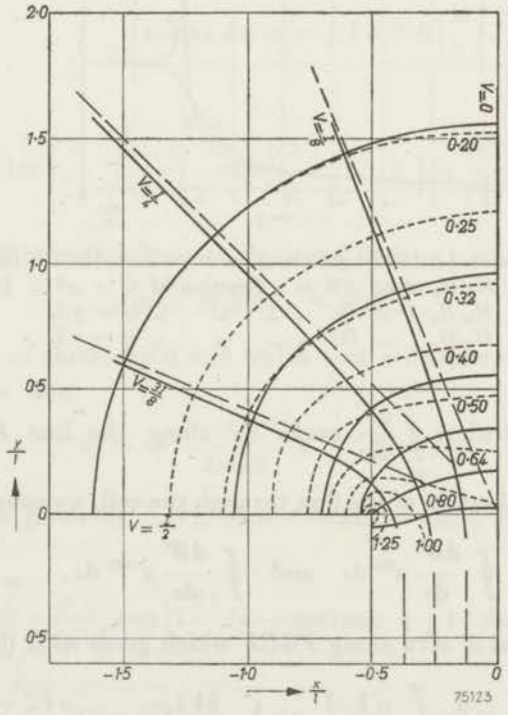

Fig. 7. Equipotentials, lines of force and lines of constant fieldstrength (dashed curves) for case *c*.

For the segments BC and DE, $\zeta > 0$ and thus $\sqrt{\zeta} = |\sqrt{\zeta}| = H_0/H$. Hence for BC

$$x = -l/2,$$

$$y = \frac{l}{\pi}\left(\frac{H_0}{H} + \tfrac{1}{2}\ln\frac{1 - H_0/H}{1 + H_0/H}\right),$$

and for DE

$$x = 0,$$

$$y = \frac{l}{\pi}\left(\frac{H_0}{H} + \tfrac{1}{2}\ln\frac{H_0/H - 1}{H_0/H + 1}\right).$$

Fig. 8 gives the fieldstrength along the boundary computed with these formulae.

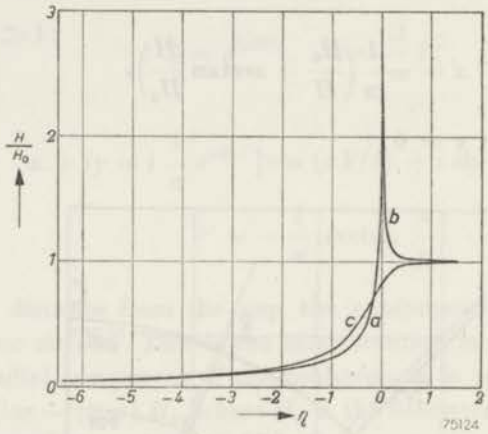

Fig. 8. Calculated fieldstrength along the boundary $ABCDE$ (fig. 6).
(a). H_y/H_0 along AB as a function of $\eta = x/l + \frac{1}{2}$,
(b). H_x/H_0 „ BC „ „ „ „ $\eta = y/l$,
(c). H_x/H_0 „ DE „ „ „ „ $\eta = y/l$.

In order to calculate $\int_{-\infty}^{0} \frac{\partial V}{\partial x} \cos kx \, dx$ along the line FG in fig. 6, needed for the evaluation of the flux through the coil, we consider

$$\oint \frac{dW}{dz} e^{ikz} dz \quad \text{and} \quad \oint \frac{dW}{dz} e^{-ikz} dz.$$

The first integral is zero along $FGEF$ which gives with (8) and (9):

$$e^{-ky} \int_{-\infty}^{0} \frac{\partial W}{\partial x} e^{ikx} dx + \frac{I}{2\pi} \int_{G'}^{\infty} \frac{1}{(\zeta - 1)} \exp\left\{-\frac{kl}{\pi}\left(\sqrt{\zeta} + \tfrac{1}{2}\ln\frac{\sqrt{\zeta} - 1}{\sqrt{\zeta} + 1}\right)\right\} d\zeta = 0.$$

Since ζ is real and greater than 1 the latter integral is real. Thus, taking the imaginary part, it follows that

$$\int_{-\infty}^{0} \frac{\partial U}{\partial x} \sin kx \, dx + \int_{-\infty}^{0} \frac{\partial V}{\partial x} \cos kx \, dx = 0. \tag{11}$$

The second integral is zero along $ABCDGFA$ which gives

$$e^{ky} \int_{-\infty}^{0} \frac{\partial W}{\partial x} e^{-ikx} \, dx = \frac{I}{2\pi} \int_{-\infty}^{C'} \frac{1}{(\zeta - 1)} \exp\left\{\frac{kl}{\pi}\left(\sqrt{\zeta} + \tfrac{1}{2} \ln \frac{\sqrt{\zeta} - 1}{\sqrt{\zeta} + 1}\right)\right\} d\zeta .$$

Taking again the imaginary part:

$$e^{ky}\left\{-\int_{-\infty}^{0} \frac{\partial U}{\partial x} \sin kx \, dx + \int_{-\infty}^{0} \frac{\partial V}{\partial x} \cos kx \, dx\right\} =$$

$$= \frac{I}{2\pi} \operatorname{Im}\left[\int_{-\infty}^{1} \frac{1}{(\zeta - 1)} \exp\left\{\frac{kl}{\pi}\left(\sqrt{\zeta} + \tfrac{1}{2} \ln \frac{\sqrt{\zeta} - 1}{\sqrt{\zeta} + 1}\right)\right\} d\zeta\right]$$

or with (11)

$$\int_{-\infty}^{0} \frac{\partial V}{\partial x} \cos kx \, dx = -\tfrac{1}{2} I e^{-ky} S\left(\frac{kl}{2}\right),$$

where

$$S(\tau) = \operatorname{Im}\left[\frac{1}{2\pi} \int_{-\infty}^{1} \frac{1}{1 - \zeta} \exp\left\{\frac{2}{\pi} \tau \left(\sqrt{\zeta} + \tfrac{1}{2} \ln \frac{\sqrt{\zeta} - 1}{\sqrt{\zeta} + 1}\right)\right\} d\zeta\right].$$

Following eq. (1) the flux from an element b dy is

$$d\Phi = M_0 b \, dy \, e^{-ky} \, S(kl/2).$$

Thence a tape of thickness d and width b at a distance a from a head of type c gives a flux

$$\Phi = \Phi' \frac{1 - e^{-2\pi d/\lambda}}{2\pi d/\lambda} e^{-2\pi a/\lambda} S(\pi l/\lambda). \tag{13}$$

The gap loss is given by $S(\tau)$, with $\tau = kl/2 = \pi l/\lambda$. For $S(\tau)$ we may write

$$S(\tau) = \operatorname{Im} \frac{1}{\pi} \int_{0}^{\infty} \frac{u}{1 + u^2} \exp\left\{i \frac{2\tau}{\pi} (u - \operatorname{arctan} u + \frac{\pi}{2})\right\} du +$$

$$+ \operatorname{Im} \frac{1}{\pi} \int_{0}^{1} \frac{u}{1 - u^2} \exp\left\{\frac{2\tau}{\pi}\left(u + \tfrac{1}{2} \ln \frac{1 - u}{1 + u} + i \frac{\pi}{2}\right)\right\} du, \tag{14}$$

or

$$S(\tau) = \frac{1}{\pi} \int_0^{\pi/2} \tan \Phi \sin \left\{ \frac{2}{\pi} \tau \left(\tan \Phi - \Phi + \frac{\pi}{2} \right) \right\} \mathrm{d}\Phi +$$

$$+ \frac{1}{\pi} \sin \tau \int_0^1 \frac{u}{1-u^2} \exp \left\{ \frac{2}{\pi} \tau \left(u + \tfrac{1}{2} \ln \frac{1-u}{1+u} \right) \right\} \mathrm{d}u . \qquad (15)$$

For large values of τ the main contribution to these integrals comes from small values of the argument. In the first integral of (15) this is true because $\sin \{(2\tau/\pi) (\tan \Phi - \Phi + \pi/2)\}$ becomes a rapidly oscillating function if $(2\tau/\pi) \tan \Phi > \pi/2$ thus giving no contribution to the integral, while in the second integral

$$u + \tfrac{1}{2} \ln \frac{1-u}{1+u} = -\frac{u^3}{3} - \frac{u^5}{5} - \ldots$$

is always negative and approaches $-\infty$ for $u \to 1$, therefore also giving no contribution to the integral if $(2\tau/\pi)\, u^3/3 \gg 1$. Hence eq.(14) may be written

$$S(\pi) = \frac{1}{\pi} \operatorname{Im} \int_0^{\infty} u \left(1 - u^2 + u^4 \ldots\right) \exp \left\{ i \frac{2}{\pi} \tau \left(\frac{\pi}{2} - \frac{u^3}{3} - \frac{u^5}{5} - \ldots \right) \right\} \mathrm{d}u$$

$$+ \frac{1}{\pi} \operatorname{Im} \int_0^{\pi/2} u \left(1 + u^2 + u^4 \ldots\right) \exp \left\{ \frac{2}{\pi} \tau \left(i \frac{\pi}{2} - \frac{u^3}{3} - \frac{u^5}{5} - \ldots \right) \right\} \mathrm{d}u .$$

Extension of the upper limit in the second integral to ∞ gives a negligible contribution to the integral. Therefore, developing for powers of u and making use of the relation

$$\int_0^{\infty} x^p \exp(-w x^q)\, \mathrm{d}x = \frac{1}{q} \frac{\Gamma\{(p+1)/q\}}{(p+1)/q}$$

the asymptotic expansion

$$S(\tau) \sim \frac{3^{1/6} \Gamma(^2/_3)}{\pi (2\tau/\pi)^{2/3}} \sin(\tau + \pi/6) + \frac{3^{5/6} \Gamma(^1/_3)}{\pi (2\tau/\pi)^{1/3}} \sin(\tau - \pi/6) + 0(\tau^{-5/6}) \quad (15a)^*)$$

is found.

The above expansion is obtained by developing eq. (14) for small values

---

*) In the course of this work The Mathematical Centre at Amsterdam also verified eq. (15*a*) by a more rigorous analysis.

of u, and therefore of ζ. Since the region round $\zeta = 0$ is mapped on the edge of the gap this means physically that only elements of the tape close to this edge are considered. Therefore the leading term of the expansion (15a) can also be arrived at by expressing $\partial V/\partial x$ in x for small values of ζ and then according to eq. (6) evaluating

$$\int_{-l/2}^{0} \frac{\partial V}{\partial x} \cos kx \, dx .$$

Eq. (8) gives in first approximation

$$z = -\frac{l}{2} - \frac{il}{3\pi} \zeta^{3/2}.$$

In order to move along BO the argument of $\zeta = re^{i\varphi}$ has to be taken $\varphi = \pi/3$ which means that in fig. 6 the representation on the ζ-plane of the line OA in the z-plane makes an angle $\pi/3$ with the ξ-axis. Thus $x = -l/2 + (l/3\pi) r^{3/2}$.

Since $\dfrac{dW}{dz} = -i(I/l)/\sqrt{\zeta}$ (eq. 10) it follows that

$$\frac{\partial V}{\partial x} = -\frac{I}{l} \operatorname{Re} \frac{1}{\sqrt{\zeta}} = -\frac{I}{l} r^{-1/2} \cos \frac{\pi}{6} = -\frac{I}{l^{3/2}} \frac{3^{1/4}}{2\pi^{1/2}} \left(x + \frac{l}{2}\right)^{-1/2}$$

and

$$\int_{-l/2}^{0} \frac{\partial V}{\partial x} \cos kx \, dx = -\frac{I}{l^{3/2}} \frac{3^{1/4}}{2\pi^{1/2}} \int_{-l/2}^{0} \frac{\cos kx}{(x + l/2)^{1/2}} \, dx ,$$

where

$$\int_{-l/2}^{0} \frac{\cos kx}{(x + l/2)^{1/2}} \, dx \approx \int_{0}^{\infty} \cos \{k(x - l/2)\} \, x^{-1/2} \, dx = \operatorname{Re} \int_{0}^{\infty} e^{ikx - ik\,l/2} \, x^{-1/2} \, dx =$$

$$= \operatorname{Re} e^{-ik\,l/2} \int_{0}^{\infty} e^{-ky} \, (iy)^{-1/2} \, i dy = \frac{\Gamma(1/2)}{k^{1/2}} \sin \left(\frac{kl}{2} + \frac{\pi}{6}\right),$$

it follows that

$$S\left(\frac{kl}{2}\right) = -\frac{2}{I} \int_{-l/2}^{0} \frac{\partial V}{\partial x} \cos kx \, dx = \frac{3^{1/4} \Gamma(1/2)}{\pi^{1/2}} \frac{\sin (kl/2 + \pi/6)}{(kl)^{1/2}}$$

which is the leading term of (15a).

For smaller values of τ, $S(\tau)$ can be computed numerically. In the next table the values of $S(\tau)$ as computed by The Mathematical Centre at Amsterdam are given for $0 < \tau < 5\pi$. Column 3 gives the values obtained by using the first two terms of eq. (15a), and column 4 those of the first term.

TABLE I

Values of $S(\tau)$ for $0 \leqslant \tau \leqslant 5$, as computed according to different formulae.

τ/π	$S(\tau)$	1st and 2nd term of (15a)	1st term of (15a)
0·000	1		
0·125	0·969		
0·250	0·880		
0·375	0·740		
0·50	0·565	0·571	
0·75	0·180	0·182	
1·00	—0·135	—0·135	
1·25	—0·282	—0·282	
1·50	—0·244	—0·244	
1·75	—0·084	—0·084	
2·00	0·091	0·092	
2·25	0·188	0·188	
2·50	0·167	0·167	
2·75	0·057	0·057	
3·00	—0·072	—0·071	—0·078
3·25		—0·147	—0·144
3·50		—0·132	—0·123
3·75		—0·044	—0·035
4·00		0·061	0·065
4·25		0·122	0·120
4·50		0·110	0·103
4·75		0·037	0·030
5·00		—0·053	—0·056

It is seen from the table that from $\tau = 0{\cdot}5\pi$ onwards the approximation by the first two terms is very satisfactory, while from $\tau = 5\pi$ onwards, that is past the fifth zero, the approximation by the first term is reasonable.

The gap loss $S\,(\pi l/\lambda)$ as a function of l/λ is represented in fig. 9. It is seen that, as could be expected on physical grounds, the gap-loss function for a head of type *c* is intermediate between those for type *a* and *b*.

Equations (2), (7) and (13) give the output for the three types of head in the case of a longitudinally magnetized tape. For perpendicular magnetization a head of type *a* gives no response as may be seen from the symmetry, whereas for the other heads the output is still given by equations (7) and (13). We proceed to prove this.

In order to apply the reciprocity theorem to perpendicular magnetization we have first to ask for the flux through an element $b\,dx$, lying in the plane of the tape. This flux is given by $-\mu_0\,(\partial V/\partial y)\,b\,dx$. Thus, applying the reciprocity theorem in the same way as above, we find for the flux through the coil of a reproducing head from a tape magnetized according to $M_y = M_0 \sin kx$, $M_x = M_z = 0$

$$d\Phi = \frac{-M_0}{I}\, b\, dy \int_{-\infty}^{+\infty} \frac{\partial V}{\partial y} \sin kx\, dx\,.$$

Here the contributions from a cosine term in the magnetization cancel each other out.

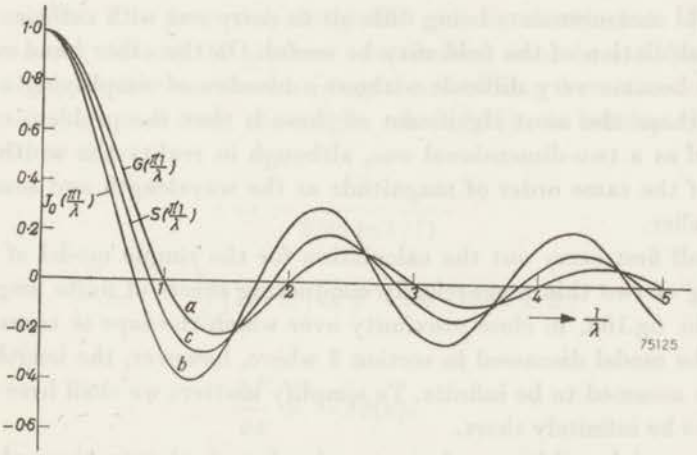

Fig. 9. The three gap-loss functions $G(\pi l/\lambda)$, $J_0(\pi l/\lambda)$ and $S(\pi l/\lambda)$ as a function of l/λ for heads of types a, b and c respectively.

Since $\partial V/\partial y = 0$ in the gap of a head of type a the output is zero for this type. For types b and c, however it follows from the fact that V is an analytical function that $\partial V/\partial y = \partial U/\partial x$. Putting in eq.(4) $dW/dz = \partial U/\partial x + i\,\partial V/\partial x$ and taking the imaginary part yields

$$\int_{-\infty}^{+\infty} \frac{\partial U}{\partial x} \sin kx\, dx = \int_{-\infty}^{+\infty} \frac{\partial V}{\partial x} \cos kx\, dx\,,$$

whence

$$d\Phi = \frac{M_0}{I}\, b\, dy \int_{-\infty}^{+\infty} \frac{\partial V}{\partial x} \cos kx\, dx\,.$$

This is eq.(1) with opposite sign.

5. Reproduction at long wavelengths

Until now we have assumed that the reproducing head is long compared with the wavelength to be reproduced. In practice this will not always be so, and, as a consequence, deviations from the predicted frequency characteristic may occur at low frequencies.

In order to determine the influence of the finite length of the head we can proceed along the same lines as above for the influence of the finite gap length. First we determine the field distribution around an energized head of finite length and then calculate the flux from a magnetized tape by application of the reciprocity theorem. This in fact was the method followed by Clark and Merrill [14]) who determined the field distribution by direct measurement.

The field measurements being difficult to carry out with sufficient accuracy, a calculation of the field may be useful. On the other hand such calculations become very difficult without a number of simplifying assumptions. Perhaps the most significant of these is that the problem can still be treated as a two-dimensional one, although in reality the width of the head is of the same order of magnitude as the wavelength and sometimes even smaller.

We shall first carry out the calculation for the simple model of a head consisting of two thin magnetically conducting sheets of finite length, AO and OB in fig.10*a*, in close proximity over which the tape is transported. This is the model discussed in section 3 where, however, the length of the head was assumed to be infinite. To simplify matters we shall here assume the gap to be infinitely short.

The potential problem we have to solve here is that in the z-plane AO be at a potential $I/2$ and OB at $-I/2$. Carrying out an inversion with centre in the origin, and inversion radius $L/2$, $z'z = (L/2)^2$, gives in the

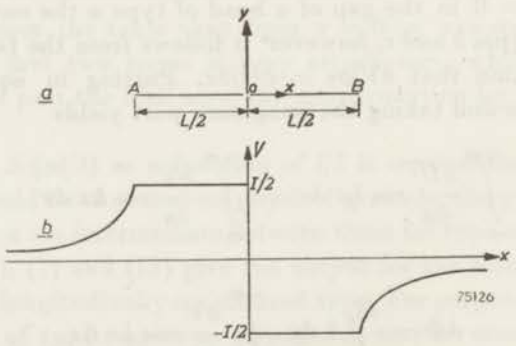

Fig. 10. *a*. Schematization of a thin head of finite dimensions. *b*. Distribution of the potential along the x-axis.

z'-plane the boundary condition that the potential V be $I/2$ from $x' = -\infty$ to $L/2$ and $-I/2$ from $x' = L/2$ to $+\infty$. The solution to this problem is given by eq.(3), whence the transformation satisfying our problem is found to be

$$z = -i\,\frac{L}{2}\,\frac{1}{\sinh\,(\pi\,W/I)}.$$

In order to calculate the flux through a coil, wound round a connecting element of the two pole-pieces, we can apply eq.(1) and calculate therefore

$$\int \frac{\partial V}{\partial x}\,\cos kx\,\mathrm{d}x$$

along the x-axis. The potential along this axis is sketched in fig.10b. Integration along AO and OB gives no contribution since here $\partial V/\partial x = 0$. Therefore the contributions to this integral are coming from the line segments outside AB, and from the origin, where $\partial V/\partial x$ is infinite. Outside AB, $U = 0$, so that

$$x = -\frac{L}{2\sin\,(\pi V/I)}.$$

Hence

$$\frac{\partial V}{\partial x} = \frac{IL}{2\pi}\,\frac{1}{x^2}\,(1-L^2/4x^2)^{-1/2} \text{ for } |x| \geqslant L/2\,.$$

In the origin

$$\frac{\partial V}{\partial x} = -\,I\delta(x),$$

where δ is the Dirac delta function.

Therefore, the flux in the coil is found to be

$$\Phi = \Phi_0\left(1-\frac{2}{\pi}\int_1^\infty \frac{\cos\beta\tau}{\sqrt{\tau^2-1}}\,\frac{\mathrm{d}\tau}{\tau}\right), \tag{16}$$

where $\beta = kL/2 = \pi L/\lambda$ and $\Phi_0 = M_0\,bd$ is the amplitude of the flux variations in the tape. The integral can be transformed by differentiating with respect to β, which gives

$$-\int_1^\infty \frac{\sin\beta\tau}{\sqrt{\tau^2-1}}\,\mathrm{d}\tau = -\frac{\pi}{2}\,J_0(\beta).\ ^{15})$$

Hence

$$\frac{2}{\pi}\int_1^\infty \frac{\cos\beta\tau}{\sqrt{\tau^2-1}}\,\frac{\mathrm{d}\tau}{\tau} = -\int_0^\beta J_0(x)\,\mathrm{d}x + c\,.$$

Since for $\beta = 0$ the first integral of this equation is 1 and and the second 0 it follows that $c = 1$, and therefore

$$\Phi/\Phi_0 = \int_0^{\pi L/\lambda} J_0(x)\, \mathrm{d}x, \tag{17}$$

which is a tabulated function [16]).

An approximation of this result can be obtained by noting that in eq. (16) the main contribution to the integral comes from $\tau \approx 1$. This is especially true for large values of β since then the contributions to the integral coming from larger values of τ cancel each other out owing to the fluctuating character of $\cos\beta\tau$. Therefore

$$\int_1^\infty \frac{\cos\beta\tau}{\sqrt{\tau^2-1}}\,\frac{\mathrm{d}\tau}{\tau} \approx \int_0^\infty \frac{\cos\{\beta(1+k)\}}{2^{1/2}k^{1/2}}\,\mathrm{d}k = \frac{\sqrt{\pi}}{\beta^{1/2}}\cos(\beta+\pi/4)$$

and hence

$$\Phi/\Phi_0 \approx 1 - \frac{2^{1/2}}{\pi(L/\lambda)^{1/2}}\cos\{\pi(L/\lambda+\tfrac{1}{4})\}. \tag{17a}$$

From fig.11, giving Φ/Φ_0 computed from eq.(17) (full line) and from (17a) (dashed line) it is seen that the approximation is excellent for values of $L/\lambda > 1$.

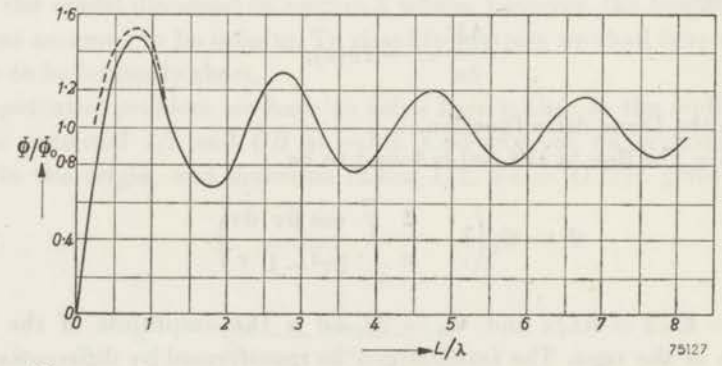

Fig. 11. $\int_0^{\pi L/\lambda} J_0(x)\mathrm{d}x$ as a function of L/λ (full line) and the approximation of this integral by $1 - 0{\cdot}45\,\dfrac{\cos[\pi(L/\lambda + 1/4)]}{(L/\lambda)^{1/2}}$ (dashed line).

We can now proceed to calculate in the same approximation the more realistic case that the edges of the pole-pieces where the tape approaches and leaves the head, A and B in fig. 12, are 90° and not 180° as in the preceding case.

Application of the theorem of Christoffel and Schwarz leads to the equation transforming the contour *CAOBD* into the ξ-axis of a ζ-plane:

$$z = \frac{L}{\pi} \{ \zeta \sqrt{1-\zeta^2} + \arcsin \zeta \}.$$

Here the main value of the arcsin has to be taken, and that value of the root that is positive in the origin.

The edges A and B are mapped on $\zeta = -1$ and $\zeta = +1$ in the ζ-plane respectively.

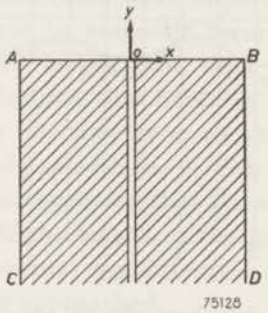

Fig. 12. Schematization of a finite head with 90° edges.

On the other hand, the equation

$$W = \frac{I}{\pi} \ln \zeta - \frac{iI}{2}$$

transforms a W-plane ($W = U + iV$) on the ζ-plane such that $V = +I/2$ is mapped on the negative and $V = -I/2$ on the positive ξ-axis.

From these equations it is found that the fieldstrength at the edge B is in first approximation

$$-\frac{\partial V}{\partial x} \approx -\frac{I}{L^{3/2}} \frac{3^{1/4}}{2^{3/2}\pi^{1/2}} \frac{1}{(x-L/2)^{1/2}},$$

so that the required integral is

$$\int_{L/2}^{\infty} \frac{\partial V}{\partial x} \cos kx \, dx \approx I \frac{3^{1/4}}{2^{3/2}\pi^{1/2}} \frac{\Gamma(3/2)}{(kL)^{3/2}} \cos\left(\frac{kL}{2} + \frac{\pi}{6}\right).$$

Hence the total flux through the head resulting from the contributions of the gap and the two edges is

$$\frac{\Phi}{\Phi_0} \approx 1 - \frac{3^{1/6}}{\pi 2^{4/3}} \frac{\Gamma(^2/_3)}{(L/\lambda)^{2/3}} \cos\left\{\pi\left(\frac{L}{\lambda} + \frac{1}{6}\right)\right\} = 1 - 0{\cdot}205 \frac{\cos\left\{\pi(L/\lambda + 1/6)\right\}}{(L/\lambda)^{2/3}}. \quad (18)$$

In fig. 13 Φ/Φ_0 according to (18) is plotted (full line) together with two measured response curves. For the first of these (dashed line) the tape was led immediately over the edges of the head. Apart from the fact that the zero's are shifted to lower values of L/λ there is good agreement with the theoretical curve. The difference may be due to the non-validity of the assumption that the head is broad compared with the wavelength.

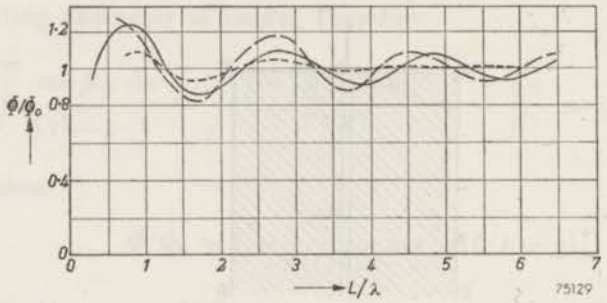

Fig. 13. Calculated output for a finite head with 90° edges (full line) and measured curve for the case that the tape is led immediately over the edges (dashed line) and at a distance of 2 mm from the edges (dotted line).

In the other case (dotted line) the tape was led in a straight line in front of the head, touching the head only at the place of the gap. Owing to the receding angles of the front planes the tape now passes the edges of the head at a certain distance, the influence of which may be described in first approximation by addition of a factor $\exp(-2\pi a/\lambda)$ to the last term of eq. (18), where a is the distance between tape and edge. This effects an increased damping of the oscillations in conformity with the measurements.

6. Discussion

In our analysis we supposed the permeability of the tape to be unity. A general solution for the case of a permeability other than unity cannot be given. For a special case, viz. $\mu = 3$ and a gap length equal to the thickness of the tape, a graphical solution was given by Begun [17]).

Our calculations show that for the three types of head discussed the factors describing the influence of tape thickness, space between tape and head, and gap length are occurring separately. For the "open" heads, types *b* and *c* of fig. 4, the influence of the first two is for longitudinal and perpendicular magnetization given by

$$\frac{1-e^{-2\pi d/\lambda}}{2\pi d/\lambda} e^{-2\pi a/\lambda}.$$

The same expression was deduced by Wallace [12]) in a different way. In both derivations, however, the assumption is made that the permeability of the tape equals unity. We shall see in Part IV that for a tape of higher permeability the expression becomes more complicated.

The gap-loss formula $\sin(\pi l/\lambda)/(\pi l/\lambda)$ is valid only in the theoretical case of a head of type *a*. For the more realistic types *b* and *c* the general behaviour, i.e. an oscillating function with decreasing amplitude, is the same. But the existing differences have important consequences for some frequently used procedures in magnetic recording. Thus it is common practice to deduce the gap length from tape velocity and frequency of the first zero, in the supposition that here $l = \lambda$. Fig. 9 shows that, for a type *c* head, $l = 0{\cdot}9\lambda$ for the first zero, so that the actual gap is 10% smaller than the calculated gap with $l = \lambda$. This is confirmed by the measurements of Lübeck [10]) who concluded that the magnetic gap is 10% longer than the mechanic gap. If the length of the gap is comparable with the depth (wide-gap measurements) the difference may become even greater; for then a head of type *b* is approached.

It has been proposed [18]) to use wide-gap measurements as a means to determine the actual flux in the tape. Then the successive maxima of the voltage across the open terminals of a reproducing head, which occur if the frequency is gradually increased, are measured, and the recorded flux in the maxima is put proportional to this voltage. The latter is only true, however, if the gap loss formula G is valid, for then, since the open voltage is proportional to the frequency, the voltage over a one-turn coil is given by

$$E = \omega \Phi G(\pi l/\lambda) = 2\pi \frac{v}{\lambda} \frac{\sin \pi l/\lambda}{\pi l/\lambda} \Phi,$$

where Φ is the recorded flux. Therefore in the extremes, where $|\sin(\pi l/\lambda)| = 1$,

$$E_m = \frac{2v}{l} \Phi,$$

independent of the wavelength.

If, however, the measurements are carried out with a head of type *c*, as is normally done, the gap-loss function $S(\pi l/\lambda)$ has to be used. Then the voltage induced by a thin tape in close contact with the head is given approximately by

$$E'_m \approx \frac{3^{1/3}\Gamma(^2/_3)}{2^{2/3}} \left(\frac{l}{\lambda}\right)^{1/3} \frac{2v}{l} \Phi \approx 1{\cdot}023 \left(\frac{l}{\lambda}\right)^{1/3} \frac{2v}{l} \Phi,$$

rising, therefore, with respect to the former formula as $(l/\lambda)^{1/3} \sim \omega^{1/3}$, or 2 dB per octave. The calculated dependence of the voltage on l/λ for a constant amplitude of the flux in the tape is given in fig. 14.

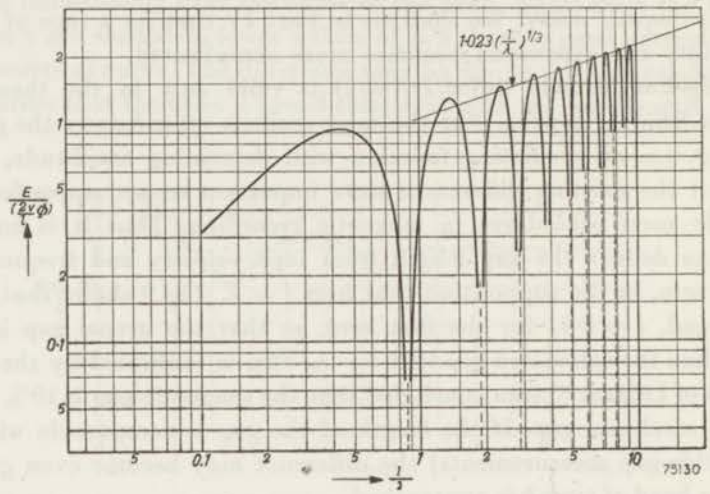

Fig. 14. Calculated output for wide-gap measurements with a semi-infinite gap.

Further it must be remembered that, although in wide-gap measurements the gap is long compared with the wavelength, the dependence of the output voltage on the space between head and tape is the same as in the case of a narrow gap, being given in both cases by the formula $\exp(-2\pi a/\lambda)$.

Recently Schmidbauer [10]) has also derived the 2dB/octave rise. He arrives at an approximate formula for the gap loss analogous in behaviour to our function $S(\pi l/\lambda)$. An expression is also given for the long-wave deviations of the frequency characteristic due to the finite length of the reproducing head, that qualitatively explains the experiments.

In another recent publication Mankin [20]) discussed these deviations, under the name of interference effects, by comparing the head with a multiplicity of gaps each acting as a source of flux. The edges of the head act as such sources. This is in conformity with our formula (1) since at the edges $\partial V/\partial x$ is large and will, therefore, give a large contribution to the integral and thus to the reproduced flux.

III. THE RECORDING PROCESS

1. Description of the d.c. and a.c. biasing method

In recording sound the first demand is that there be a perfect linear relation between the output and the input signal. If the recording characteristic is not linear this becomes apparent by the creation of harmonics or combination tones to which the human ear is very sensitive, specially to the latter.

In principle it should be possible to obtain a linear recording even without the aid of a special biasing field. The normal magnetiziation curve of a virgin magnetic material in fact has a point of inflection in the origin; by making the amplitude of the signal sufficiently small a region around the origin can be found, that is sufficiently linear. In this region, however, the magnetic processes are for the major part reversible, so that the slope of the remanent virgin curve is practically zero. Because of the weakness of the recorded signal the ratio of the signal to the unavoidable background noise becomes too unfavourable.

An extension of the linear portion of the recording characteristic can be obtained either by the direct current or by the alternating current biasing method.

In the d.c. method the tape is magnetized to saturation (B in fig. 15) by a separate head. This head acts at the same time as an erasing head, for by bringing the tape to saturation anything that might have been recorded on it is obliterated. Leaving this head the tape has reached the remanent magnetization M_R. During the recording a magnetic field is added to the signal field to be recorded. The polarity of this biasing field is opposite to the field that has previously brought the tape to magnetization, and the magnitude is of the order of the coercive force, thus bringing the magnetization to a point C when no signal field is applied. If the biasing field is chosen such that C coincides with a point of inflection of the hysteresis loop, a region around C is essentially linear and has a much steeper slope and, therefore, a much greater amplitude of the recorded magnetization than the linear part of the virgin magnetization curve around the origin. After leaving the recording head the magnetization reaches the M-axis along a branch of the minor hysteresis loop, for instance DD' or CC'. These branches being essentially parallel the remanent magnetization remains a linear function of the applied signal field.

In the alternating current biasing method an a.c. field of an amplitude approximately equal to the coercive force and a frequency well above the highest to be recorded is superimposed on the signal field. It appears that in this way too a linearization of the recording characteristic is achieved Compared with the d.c. method the a.c. method has two advantages.

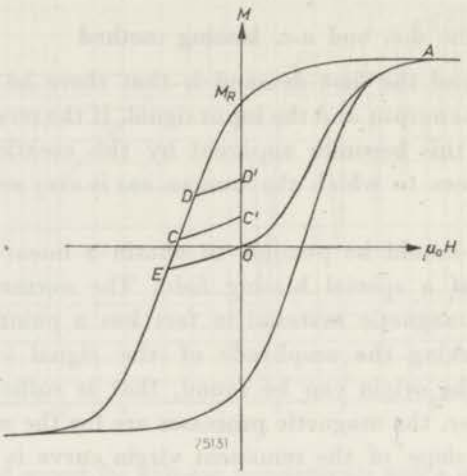

Fig. 15. Schematization of the d.c. recording method.

Firstly, in the absence of a signal the tape leaves the recording head in a demagnetized state. The fluctuations of the flux being less for a demagnetized than for a magnetized tape this means that for an a.c. biased tape the background noise is less than for a d.c. biased tape. Secondly, the linear range of the recording characteristic is more extended in case of a.c. biasing, which means that the a.c. biasing method results in a greatly improved signal-to-noise ratio.

In principle it should also be possible to choose the direct current bias such that a point E in fig. 15 is reached under the influence of this biasing field and the origin after this field has faded. But the point E does not necessarily coincide with the point of inflexion C, and if not, this limits the recording range. Further a careful adjustment of this bias is necessary, and, owing to the inhomogeneity of the field in front of the recording head, the appropriate value is only reached for a small layer of the tape. Finally, even if the tape as a whole reaches the origin in this way, the state it has thus acquired is different from the virgin demagnetized state.

Owing to these reasons the improvement of the signal-to-noise ratio for direct current recording, if possible at all, is very difficult to achieve.

2. Current explanations of the a.c. biasing method

An explanation of the a.c. biasing method, was first given by Camras [21]), and independently along the same lines by Toomin and Wildfeuer [22]), the latter supporting it by an oscillographic study. Their explanation runs as follows: if the amplitude of the a.c. biasing field is such that a minor hysteresis loop is followed that has its reversal points on the steep branches of the major loop, than the application of an additional direct field will result in the shift of the minor loop along the steep branch. In fig. 16 a field H_1 will shift the loop $ABCD$ to the loop $A'B'C'D'$. Because the flanks of the major hysteresis loop are linear over a considerable length, the shift of the minor loops is proportional to the direct field applied.

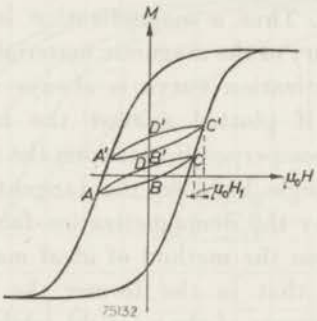

Fig. 16. Schematization of the a.c. recording method.

If now in the case of the loop $A'B'C'D'$ the a.c. field decreases, a path will be traced lying inside this loop and resulting in a magnetization about halfway between B' and D' when the a.c. field as well as the direct field have completely faded. This remanent magnetization too will be a linear function of the applied direct field.

In the above explanation it is assumed that stationary minor loops are followed. This, however, is only the case if a large number of cycli of the a.c. field are traversed while the direct field remains constant. In front of an actual head the fieldstrength varies rapidly with the distance to the gap, so that for a tape passing the head this condition is not fulfilled. To avoid this difficulty Holmes and Clark [23]) give an explanation in which they try to follow the magnetizing forces for successive parts of the tape more in detail. The magnetization curves, however, are insufficiently known to predict the ultimate magnetzation of the tape with the desired accuracy. To come to conclusions a comparison is made with an AB-class push-pull amplifier, a method which yields the same results

as those discussed above but has the disadvantage that the physical processes are less easily understood.

Both explanations are based upon properties of the magnetization curve without entering into the physcial processes underlying these properties.

3. Relation between a.c. and ideal magnetization

Before discussing a physical model that explains the linearizing effect of an a.c. bias, we wish to draw attention to the close relation that exists between the method of a.c. biasing and the process of ideal or anhysteresic magnetization as proposed by Steinhaus and Gumlich [24]). In this method magnetization is accomplished by superimposing on the magnetic field an a.c. field of sufficiently large amplitude and then gradually decreasing this amplitude to zero. Thus a magnetization is brought about that is independent of the history of the magnetic material. Lying above the virgin curve, the ideal magnetization curve is always concave with respect to the H-axis. Further, if plotted against the internal field, the ideal magnetization curve rises perpendicular from the origin. If plotted against the external field the angle between the tangent in the origin and the M-axis is determined by the demagnetization-factor.

The difference between the method of ideal magnetization and that in magnetic recording is, that in the former the magnetic field remains constant during the decrease of the a.c. field, while in the latter it decreases at the same rate.

This may be illustrated by figs 17 and 18, taken from unpublished

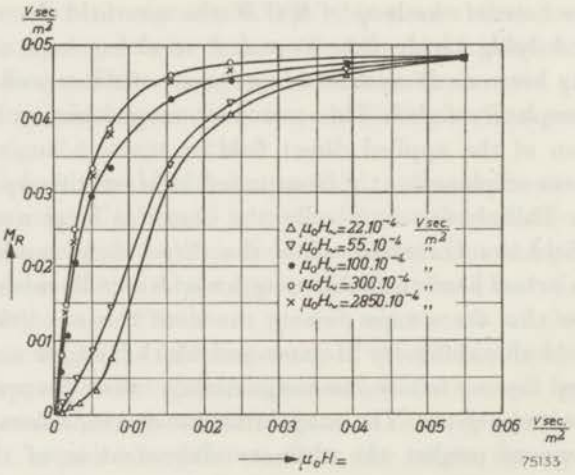

Fig. 17. Remanent magnetization as a function of direct field if an idealization process has been carried out starting from the indicated peak value of the idealizing field.

measurements of Dr J. J. Went on magnetic tapes in homogeneous fields. The coercive force of the tape in question was $\mu_0 H_c = 75 \cdot 10^{-4}$ Vsec/m^2 In both figures the remanent magnetization after the tape has been subjected to a superposition of a direct field and an a.c. field is plotted against the direct field for different values of the a.c. field. But, whereas in fig.17 the a.c. field was first removed and then the direct field, as in the case of ideal magnetization, in fig.18 both were reduced simultaneously and at the same rate, as is the case in magnetic recording. Experimentally this is achieved by drawing the tape out of a coil fed by superposed direct and alternating currents.

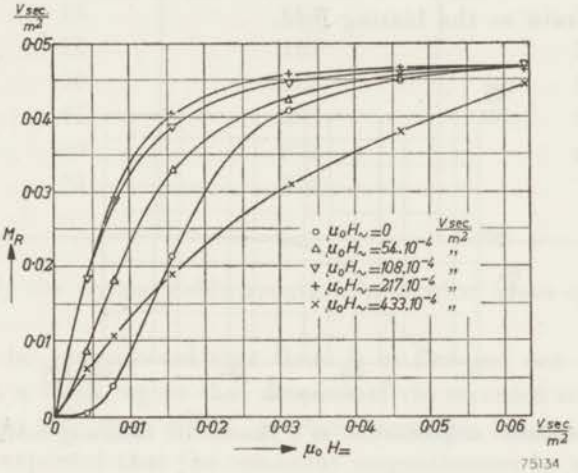

Fig.18. Remanent magnetization for the case where the direct field decreases at the same rate as the idealizing field, as a function of the starting value of the direct field.

It is seen from fig.17 that as the initial value of the a.c. field increases, the remanent magnetization increases also but approaches more and more a limiting value, the ideal curve. For a value of $\mu_0 H = 300.10^{-4}$ Vsec/m^2 the remanent curve already coincides with the ideal curve. In fig.19 the remanent magnetization is plotted against the idealizing fieldstrength, for a smal value of the direct field. It appears that the steepest part of this curve, at $\mu_0 H_c = 75.10^{-4}$ Vsec/m^2, coincides with the coercive force of the tape in question.

Comparison of figs. 17 and 18 shows that in the latter the magnetization obtained is always smaller than in the former. This is to be expected, for in the latter case the direct field is smaller than in the former during all stages of the recording process.

It further appears that according to both methods an increase of the alternating field results in a better linear departure from the origin, but

that in the latter case the magnetization does not tend towards a limiting value for high biasing fields. Instead, from a certain value of this field onwards, the magnetization decreases with increasing biasing field. This is illustrated in fig. 20, giving for a small value of the direct field the dependence of the remanent magnetization on the biasing field. The decrease of the magnetization is explained if we assume that there is only a certain range of biasing fieldstrengths that determines what magnetization is ultimately recorded under the combined action of a.c. and d.c. field. For if, in that case, we start with a high value of the a.c. field the magnetization is recorded at the time the decreasing a.c. field passes this critical range, and the direct field at that time has decreased at the same rate as the biasing field.

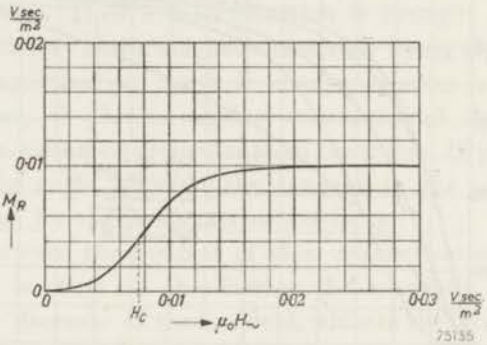

Fig.19. Remanent magnetization as a function of idealizing fieldstrength.

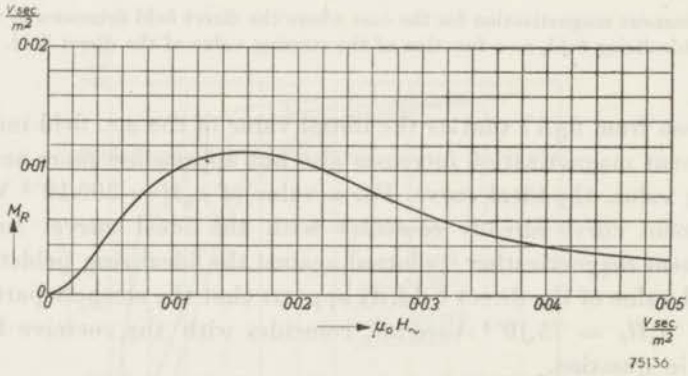

Fig.20. Remanent magnetization for the case where the direct field decreases with the idealizing field.

To estimate the value of the critical fieldstrength we will compare the direct fields that result in the same magnetization for ideal and a.c. bias magnetization. If the a.c. field in the latter case is such that we are

well over the maximum of fig.20 we may expect that these fields are related as the critical fieldstrength and the starting value of the a.c. field. Thus, by comparing the ideal curve of fig.17 with the curve for $\mu_0 H_\sim = 433 \cdot 10^{-4}$ Vsec/m² of fig.18 we obtain for different magnetizations the following results.

$M_R \cdot 10^4$ Vsec/m²	$\mu_0 H_{id} \cdot 10^4$ from fig. 17 Vsec/m²	$\mu_0 H_m \cdot 10^4$ from fig. 18 for $\mu_0 H_r = 433.10^{-4}$ Vsec/m²	$\mu_0 H_{crit} \cdot 10^4 = \frac{H_{id}}{H_m} .433$ Vsec/m²
50	5	32	67
100	10	69	63
150	15	114	57
200	22	164	58
250	30	225	58
300	41	293	61
350	60	392	66
400	85	514	72

Accordingly the critical field strength is somewhat lower than the coercive force.

It should be remembered that there is in fact not one critical fieldstrength, but a small region that determines the recorded magnetization. This is evident also from fig.19. If there were one definite critical field it should be expected that the remanent magnetization be zero for idealizing fields below and have its full strength for fields above this critical value.

4. Magnetic model explaining the a.c. magnetization

We will now give a simple model that explains the ideal as well as the a.c. bias magnetization. Suppose that in a particle a number of magnetic states are possible. Each magnetic state corresponds to a minimum of the potential energy and is separated from other minima by potential barriers. For reasons of simplicity we will assume that the potential barriers are equally high, though this is not essential to our argument.

Application of a magnetic field will diminish the potential energy for those states where the direction of the magnetization is more in accordance with the direction of the field. Hence the potential barriers will decrease on the one side and increase on the other side of the potential minimum. For a certain value of the fieldstrength the first barrier will have disappeared and the magnetization will jump to a state with lower energy. Since all the barriers were supposed to be of equal height they

will all be at the same fieldstrength and therefore saturation will be obtained. Reversal of the field will effect saturation in the opposite direction. For an a.c. field of sufficient strength the magnetization will alternate between these two directions. If now the amplitude of the a.c. field is decreased gradually, there will be an equal chance for the magnetization to reach any of the potential minima. Thus a medium built up of a large number of independent particles will reach a state of zero magnetization.

If, however, a small direct field is added to the decreasing a.c. field there will be a preference for the direction of the direct field. In our case where all the potential barriers are of equal height the satured state will be reached provided only that the decrease of the a.c. field between two successive peak values is smaller than twice the strength of the direct field. Let a be the amplitude of the a.c. field at a certain moment, Δ the decrease of the a.c. field between two peaks, d the strength of the direct field and h the fieldstrength at which a potential barrier can just no longer be crossed; then the fieldstrength h will be reached for the first time when the a.c. and d.c. fields are of opposite direction, and this can just happen when $a - d = h$. When the a.c. field has altered its direction the amplitude of the next extreme will be $a - \Delta + d = h - \Delta + 2d$. This will surpass the field strength h if $\Delta < 2d$, and accordingly the potential barriers on the other side of the minimum in question will be crossed. Therefore the only final state possible is that state where saturation in the direction of the applied field has been reached.

This is the explanation given by Steinhaus and Gumlich of the ideal magnetization. In effect, in a diagram of magnetization vs. internal field, the ideal curve will rise perpendicularly from the origin.

In reality a medium is not magnetized to saturation by an arbitrarily small direct field. This is because the magnetization of the particle gives rise to a demagnetizing field opposite in direction to the external field. The magnetization will increase to that value for which the external field is completely cancelled by the demagnetizing field. For only if the internal field is zero, will no further increase of the magnetization take place during the idealizing process.

As the demagnetizing field is proportional to the magnetization and equals the direct field in strength, the residual magnetization will be proportional to the external field. The conditions to be fulfilled are that the a.c. field should be of sufficient strength for the magnetization to overcome the potential barriers for all the particles, and that there will be a sufficient number of stable positions of the magnetization.

Because the coercive force of a medium is that fieldstrength for which only half of the particles have reversed their magnetization, the first

condition viz. that all the barriers are overcome means that the idealizing field has to be well above coercivity, in accordance with fig.19. In fact it has to be above the highest coercive force met with in any of the particles.

If the number of stable magnetizations in one particle is limited, the latter condition will be fulfilled as well if the number of particles is sufficiently large.

In general we may explain the linearizing action of the a.c. field as the excitation of a magnetization which results in an internal field equal to the external field but of opposite direction.

If during the decrease of the alternating field the direct field changes also, as is the case in magnetic recording, the recorded magnetization is determined by that value of the direct field which existed at the moment that the amplitude of the alternating field was just sufficient to make the magnetization cross the potential barriers. In the case where the particles have different coercive forces, each particle will obtain the remanent magnetization that belongs to the value of the direct field existing when the a.c. field equalled its own coercive force.

5. Possible mechanisms of the magnetization process

In the above model the mechanism of the magnetization process was kept out of the discussion. It was only assumed that a number of magnetic states separated by potential barriers are possible and that these states are accompanied by a demagnetizing field proportional to the magnetization. For instance, a particle built up of two domains of different magnetization, separated by a Bloch wall that has a number of preferred positions, should match these requirements. We shall now see whether this can be brought in accordance with what is known about the magnetic particles.

From electronmicroscopic studies it appears that the particles γFe_2O_3, used in the magnetic tape studied above, are less than 0·1 μm in diameter. It depends upon the magnetic properties whether a Bloch wall can exist in these small particles, or whether it is energetically more favourable that the particle is magnetized as a whole.

The constants to be known are the Curie Temperature T_c, the lattice constant a, the saturation magnetization M_s, and the anistropy constant K. The thickness δ of a 90° wall may then be estimated from.

$$\delta = \left(\frac{kT_c}{a}\right)^{1/2} K^{-1/2},$$

and the wall energy per unit surface from

$$\sigma = \left(\frac{kT_c}{a}\right)^{1/2} K^{1/2}\ ^{25}).$$

No value for the anisotropy constant of γFe_2O_3 being available, K can be estimated from the "approach to saturation" of the magnetization curve; because, if all irreversible processes have taken place, a further increase in magnetization can be accomplished only by rotation of the magnetization against the anisotropy forces. For practically independent particles with cubic symmetry the approach to saturation is given [26]) by

$$\frac{M}{M_s} = 1 - \frac{8}{105}\left(\frac{K}{M_s}\frac{1}{H}\right)^2 - \frac{192}{5005}\left(\frac{K}{M_s}\frac{1}{H}\right)^3$$

which satisfies approximately the experimental approach (fig. 21) by insertion of $\mu_0 K/M_s = 0{\cdot}08$ Vsec/m². With $M_s = 0{\cdot}44$ Vsec/m² this yields $K = 28000$ N/m² ($= 28{\cdot}10^4$ ergs/cm³).

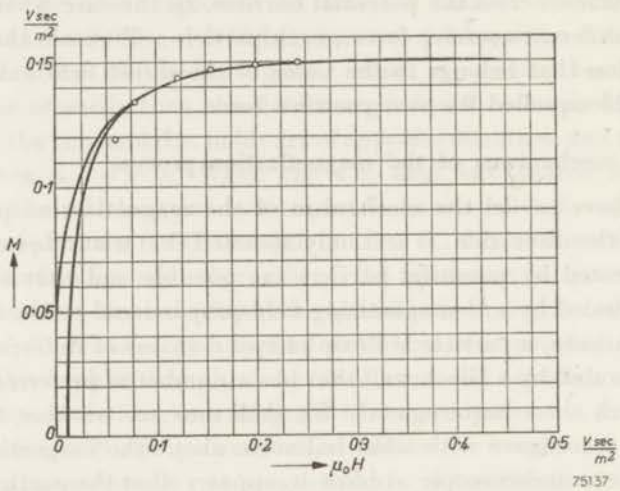

Fig. 21. Hysteresis loop with approach to saturation. The points are calculated from form. (1).

With $T_c = 1000$ °K, $a = 3$ Å the thickness of a 90° wall is $\delta = 350$ Å, and the energy $\sigma \approx 1{\cdot}2.10^{-3}$ N/m ($= 1{\cdot}2$ erg/cm²).

If a spherical particle is magnetized to saturation the magnetostatic energy density is $M_s^2/(6\,\mu_0)$ N/m² per unit volume, and thus of a particle of radius r

$$E_m = \frac{2\pi}{9} r^3 \frac{M_s^2}{\mu_0} \text{ Nm}.$$

On the other hand the introduction of two perpendicular 90° walls in the particle will introduce a configuration in which the flux path is internally closed and the magnetostatic energy consequently very small. The energy then is that of the wall, $E_w \approx 2\pi r^2\sigma$, and the critical diameter for which

the energies are equal is $r_{cr} = 750$ Å. For particles with a diameter of less than 0·15 μm the saturated configuration has the lesser energy.

It seems therefore improbable that walls should occur in the magnetic powder studied above, unless positions of the Bloch wall in the particles are possible with an energy lower than the energy according to the formula for σ given above.

If, on the other hand, the particles are magnetized to saturation a change can only be obtained by rotation from one direction of easy magnetization to another. For a spherical particle with cubic lattice the coercive force is $2K/M_s$ if the direction of the applied magnetic field is opposite to the direction of magnetization. For a medium build up of a number of such particles oriented at random the average force was calculated by Néel [27]) as 0·64 K/M_s. For the magnetic powder of the recording tape studied this should give a coercive force of $640 \cdot 10^{-4}$ Vsec/m^2 instead of the observed $75 \cdot 10^{-4}$ Vsec/m^2. Therefore, if the particles are magnetized as a whole they are either not spherical, or not independent. In the latter case clusters of particles may be imagined in which the particles influence each other in such a way that the coercive force is less than in the case of separate particles. In this cluster a demagnetizing field proportional to the magnetization will occur.

IV. CALCULATION OF THE FIELDS IN AND AROUND THE TAPE

1. Basis of the calculation

When the recording process has taken place and the tape has left the recording head the recorded magnetization will give rise to an external field but also to a demagnetizing field in the tape. This field will be directed opposite to the recorded magnetization and thus result in a decrease of the latter. This decrease will be the more pronounced the stronger the demagnetizing field and the greater the permeability of the tape. When the permeability equals unity, the magnetization will not be affected by this or any other field provided the fieldstrength does not exceed the coercive force.

In this case of unit permeability, the equations for the response curve of the preceding section hold. Here it makes no difference if the recorded magnetization is directed in the direction of motion of the tape (longitudinal magnetization) or perpendicular to the plane of the tape (perpendicular magnetization), although the demagnetizing fields are quite different in the two cases, especially for long wavelengths.

This is evident from the fact that the apparent magnetic poles which give rise to the demagnetizing field, are equal to $\mathrm{div}\boldsymbol{M}/\mu_0$. Thus for longitudinal magnetization the poles, and therefore also the demagnetizing field, tend towards zero for increasing wavelength. For perpendicular magnetization, on the contrary, there are always poles on the surface of the tape that give rise to a demagnetizing field, independent of the wavelength.

We shall now proceed to calculate the residual magnetization under the influence of the demagnetizing field of a tape in which the magnetic moment is not rigidly fixed or, in other words, that has a relative permeability greater than unity.

For the tape the Maxwell equations hold

$$\mathrm{curl}\ \boldsymbol{H} = 0\,, \tag{1}$$

$$\mathrm{div}\ \boldsymbol{B} = \mathrm{div}(\boldsymbol{M} + \mu_0\boldsymbol{H}) = 0\,. \tag{2}$$

To solve the problem a relation between $\boldsymbol{M}$ and $\boldsymbol{H}$ must be known. For this we shall use

$$\boldsymbol{M} = \boldsymbol{M}_0 + (\mu - 1)\,\mu_0\boldsymbol{H}. \tag{3}$$

For $\boldsymbol{M}_0 = 0$ this is the normal relation for linear isotropic media, where μ is the relative reversible permeability. Eq.(3) involves that after irreversible processes have taken place such that a remanent magnetization $\boldsymbol{M}_0$ is brought about, a magnetic field produces the same change in magnetization as before, independent of the magnitude of the remanent magnetization. This of course is only true in a limited range of the remanent magnetization, but it is to be expected that it holds with sufficient accuracy in the range used in magnetic recording.

A proof for the independence of the permeability of the permanent magnetization M_0 is found from the measurements of the selfinductance of a coil filled with tape. From these measurements it appears that the permeability does not change more than 2% after the tape has been subjected to direct fields, up to saturation strength.

That no irreversible changes occur may be seen from the fact that the recorded magnetization does not decrease noticeably after repeated playback. For during the passage of a head consisting of high permeable metal the demagnetizing field is decreased considerably. If irreversible processes are taking place, a decrease of $\boldsymbol{M}_0$ is to be expected. Since the voltage induced in the reproducing head is a measure for M_0 the result would be a decrease of the output voltage after repeated playback, an effect which is only observed in a slight degree after the first few times.

From eqs(1), (2) and (3) it follows that

$$\Delta \boldsymbol{H} = -\frac{1}{\mu\mu_0} \operatorname{grad} \operatorname{div} \boldsymbol{M}_0. \tag{4}$$

$\boldsymbol{M}_0$ is the magnetization recorded by the recording head. Thus, if the boundary conditions are known, $\boldsymbol{H}$ may be solved from this equation.

To make the boundary problem more easy to solve we shall suppose the tape to be of infinite length and width, the thickness of the tape being d. As we shall see the influence of the neighbourhood of a high permeable reproducing head cannot be neglected. The head is introduced by the supposition that in a plane at a distance a from the tape the lines of force are perpendicular to this plane. This is equivalent with a head of infinite dimensions and of infinite permeability with its surface in this plane, the gap of which is so small that its influence on the field distribution may be neglected.

We shall use a coordinate system with its origin in the boundary plane of the tape nearest to the head, with the x-axis in the direction of motion and the y-axis normal to the plane of the tape (fig. 22). Thus the other boundary plane of the tape is $y = -d$, and the boundary plane of the head is $y = a$.

The recorded magnetization $\boldsymbol{M}$ be sinusoidal and a function of x only. The direction of $\boldsymbol{M}$ is arbitrary in the x-y plane. In order to make the formulae less intricate we shall treat the longitudinal magnetization (directed along the x-axis) and the perpendicular (directed along y-axis) separately. The general case may be found from these two by superposition.

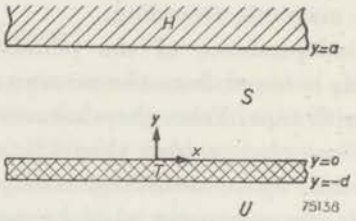

Fig.22. Schematic view of tape T and head H, the latter represented by the plane $y = a$ above which the permeability is infinite.

2. Longitudinal magnetization

The recorded magnetization being directed along the x-axis we may write for the tape

$$M_{0x} = M_0 \sin kx, \quad M_{0y} = 0; \quad (k = 2\pi/\lambda).$$

Thus eq.(4) becomes

$$\Delta H_x = \frac{M_0}{\mu\mu_0} k^2 \sin kx, \quad \Delta H_y = 0.$$

This is solved by

$$H_x = \left(A_1 e^{ky} + A_2 e^{-ky} - \frac{M_0}{\mu\mu_0}\right) \sin kx,$$

$$H_y = (-A_1 e^{ky} + A_2 e^{-ky}) \cos kx,$$

where A_1 and A_2 are arbitrary constants.

Outside the tape analogous solutions hold with $M_0 = 0$. Thus we have three sets of solutions each with two constants.

The six constants are determined by the boundary conditions

$$\begin{aligned} y = -\infty &: H_x = H_y = 0, \\ y = -d &: H_x \text{ and } B_y \text{ continuous}, \\ y = 0 &: \text{ " " " " ", } \\ y = a &: H_x = 0. \end{aligned}$$

This gives six equations for the determination of the constants. By

solving the constants and inserting the values we obtain the solution satisfying the differential equation and the boundary conditions

for $-\infty < y < -d$:

$$\begin{matrix}\mu_0 H_x \\ \mu_0 H_y\end{matrix} = \begin{matrix}-\sin kx \\ +\cos kx\end{matrix} \times \frac{M_0 \tanh kd \{\tanh ka + (1/\mu) \tanh (kd/2)\} \exp\{k(y+d)\}}{1 + \tanh ka + (\mu \tanh ka + 1/\mu) \tanh kd}; \tag{5a}$$

for $-d < y < 0$:

$$\begin{matrix}\mu\mu_0 H_x + M_0 \sin kx \\ \mu\mu_0 H_y\end{matrix} = \begin{matrix}+\sin kx \\ -\cos kx\end{matrix} \times \left\{ \begin{matrix} A & -B \\ \cosh k(y+d/2) & \cosh ky \\ \sinh k(y+d/2) & \sinh ky \end{matrix} \right\},$$

where

$$A = \frac{M_0 \{2 \cosh (kd/2) + (1/\mu) \sinh (kd/2)\}}{\cosh kd \{1 + \tanh ka + (\mu \tanh ka + 1/\mu) \tanh kd\}},$$

$$\text{and} \quad B = \frac{M_0 (1 - \tanh ka)}{\cosh kd \{1 + \tanh ka + (\mu \tanh ka + 1/\mu) \tanh kd\}}; \tag{5b}$$

for $0 < y < a$:

$$\begin{matrix}\mu_0 H_x \\ \mu_0 H_y\end{matrix} = \begin{matrix}\sin kx \sinh k(a-y) \\ \cos kx \cosh k(a-y)\end{matrix} \times \frac{-M_0 \tanh kd \{1 + (1/\mu) \tanh (kd/2)\}}{\cosh ka \{1 + \tanh ka + (\mu \tanh ka + 1/\mu) \tanh kd\}}. \tag{5c}$$

It is seen from eq.(5b) that in general, the field, and thus the magnetization in the tape, is a function of the depth in the tape. If, however, the wavelength is large in comparison with the thickness of the tape, or $|ky| < kd \ll 1$, then in first approximation

$$\mu_0 H_x \approx -M_0 kd \frac{\tanh ka}{1 + \tanh ka} \sin kx. \tag{6}$$

The field is directed against the magnetization and constant over the depth of the tape. To this approximation a demagnetization factor D can be introduced by the equation $D = -\mu_0 H_x / M_x \approx -\mu_0 H_x / M_0 \sin kx$, which with eq.(6) gives

$$D = kd \frac{\tanh ka}{1 + \tanh ka}.$$

D is inversely proportional to the wavelength and depends, moreover, on the space a between head and tape, decreasing when a decreases. For tape and head in close contact ($a = 0$) the demagnetizing factor is zero, while for a tape free in space ($a = \infty$) $D = \pi d/\lambda$.

If the wavelength is not large in comparison with the thickness of the tape, $\boldsymbol{H}$ and $\boldsymbol{M}$ are different functions of the depth in the tape, and it is therefore senseless to introduce a demagnetizing factor.

For a tape in free space the demagnetizing field has a maximum and the magnetization a minimum in the centre of the tape. This is illustrated in fig. 23*a*, giving the computed induction $B_x = M_x + \mu_0 H_x = M_0 \sin kx + \mu\mu_0 H_x$ as a function of the depth in the tape for a tape with a permeability $\mu = 4$, and for different values of $d/\lambda = kd/2\pi$. Fig. 23*b* gives the same data for a tape in close contact with the head ($a = 0$). It is seen that by the presence of the head the demagnetizing field is decreased and thus the original magnetization partly restored.

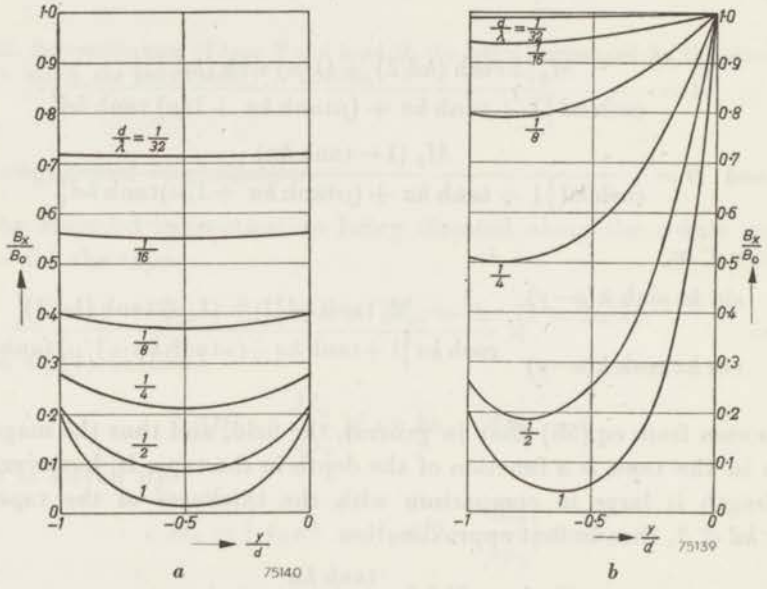

a *b*

Fig. 23. Longitudinal component of the induction in a tape of permeability $\mu = 4$. *a*. tape free in space; *b*. tape on one side ($y = 0$) in contact with a head.

It is most important to know the flux passing through the coil of the reproducing head due to the presence of the magnetized tape. This may be calculated by considering the plane $x = x_0$, where x_0 is the abscis of the (infinitely short) gap. From div $\boldsymbol{B} = 0$ it folllws that the balance of the flux traversing this plane is zero. Thus the flux in the head through this plane is found by calculating the flux in the tape and substracting the flux closing in the space under the tape, U (fig. 22), and between tape and head, s. If the head is constructed properly, then the flux through the head is forced through the coil by the reluctance of the gap.

The amplitude Φ_1 of the flux through a width b of the tape is found from

$$\Phi_1 \sin kx_0 = b \int_{-d}^{0} B_x \mathrm{d}y = b \int_{-d}^{0} (\mu\mu_0 H_x + M_0 \sin kx_0)\, \mathrm{d}y =$$
$$= \Phi_0 \frac{\tanh kd}{kd} \frac{1 + (2/\mu)\tanh (kd/2) + \tanh ka}{1 + \tanh ka + (\mu \tanh ka + 1/\mu)\tanh kd} \sin kx_0 .$$

Here $\Phi_0 = M_0 bd$ is the amplitude of the flux variations in the tape at long wavelengths. The dependence of Φ_1/Φ_0 on a/λ is represented in fig. 24.

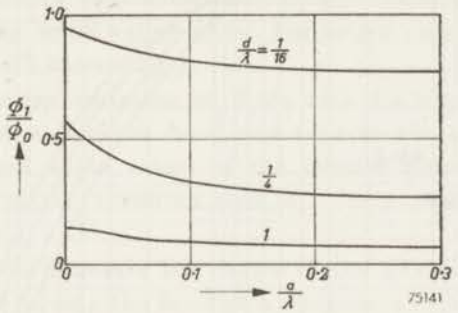

Fig. 24. Dependence of the flux in the tape on the separation between head and tape for a tape of permeability $\mu = 4$.

In the same way the flux Φ_2 below the tape is found to be

$$\Phi_2 = -\Phi_0 \frac{\tanh kd}{kd} \frac{\tanh ka + (1/\mu)\tanh (kd/2)}{1 + \tanh ka + (\mu \tanh kd + 1/\mu)\tanh kd},$$

and the flux Φ_3 closing between head and tape

$$\Phi_3 = -\Phi_0 \frac{\tanh kd}{kd} \frac{\{1 + (1/\mu)\tanh (kd/2)\}(1 - 1/\cosh ka)}{1 + \tanh ka + (\mu \tanh ka + 1/\mu)\tanh kd}.$$

Thus the flux Φ through the coil of the head is

$$\Phi = \Phi_1 - \Phi_2 - \Phi_3 =$$
$$= \Phi_0 \frac{\tanh kd}{kd} \frac{1 + (1/\mu)\tanh (kd/2)}{1 + \tanh ka + (\mu \tanh ka + 1/\mu)\tanh kd} \frac{1}{\cosh ka}. \quad (8)$$

The same result is obtained more directly by integrating the vertical component of the induction at the surface of the head from $x = 0$ to $x = x_0$. Then, however, the relative importance of the different factors that reduce the output does not stand out.

In the general formula (8) Φ depends upon d/λ, a/λ and μ in a rather complex way. For $\mu = 1$ we may write

$$\frac{\Phi}{\Phi_0} = \frac{\tanh kd}{kd} \; \frac{1+\tanh(kd/2)}{1+\tanh kd} \; \frac{1}{(1+\tanh ka)\cosh ka} = \frac{1-e^{-2\pi d/\lambda}}{2\pi d/\lambda} e^{-2\pi a/\lambda}, \quad (8a)$$

which is the expression derived in Part II.

For small values of ka and kd the first approximation of (8) gives

$$\Phi/\Phi_0 \approx 1 - ka - kd/2\mu . \quad (8b)$$

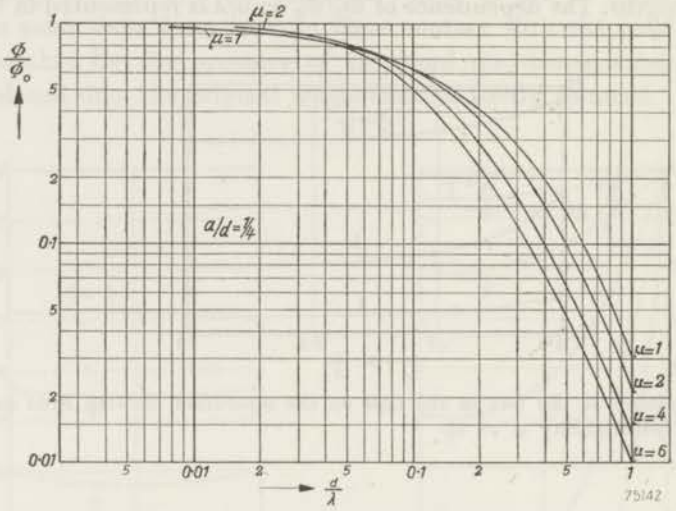

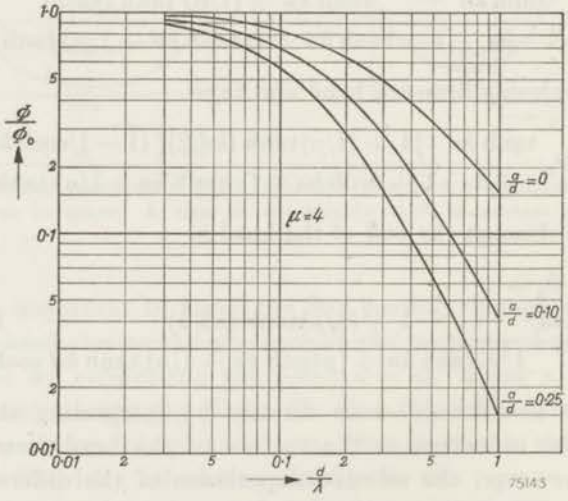

Fig. 25. Reproduced flux as a function of wavelength
a. for some values of the permeability, and a/d = ¼
b. For some values of the space between head and tape and $\mu = 4$.

For larger values of kd, $\tanh(kd/2)$ and $\tanh kd$ are approximately 1 and thus

$$\frac{\Phi}{\Phi_0} \approx \frac{1}{kd} \frac{1}{1+\mu \tanh ka} \frac{1}{\cosh ka} = \frac{1}{kd} \frac{2}{\mu+1} \frac{e^{-ka}}{1-e^{-2ka}\,(\mu-1)/(\mu+1)}. \quad (8c)$$

Since $\tanh 1{\cdot}5 = 0{\cdot}9$ this is a reasonable approximation from $d/\lambda = 0{\cdot}5$ onwards.

It is easily seen from the general formula (8) that an increase of kd and ka always results in a decrease of Φ/Φ_0. However, an increase of the permeability may sometimes enlarge the flux in the head as is seen from (8b) for small values of kd. For larger values of kd (eq.8c) the flux decreases with increasing μ.

In fig. 25*a* the variation of Φ/Φ_0 with d/λ is given for a constant ratio of the space a between head and tape to the thickness d of the tape, $a/d = \frac{1}{4}$, and some values of the relative permeability μ of the tape. Fig. 25*b* gives the variation with d/λ for a tape with $\mu = 4$ and some values of a/d.

In order to illustrate the causes of the flux loss in the case of a tape with $\mu = 4$ passing the head at a distance $a = 0{\cdot}1d$, fig. 26 represents as a function of d/λ the fraction of the flux in the tape closing beneath the tape (curve *a*) and the flux closing between tape and head (curve *b*). The remaining flux finds its way through the head (curve *c*).

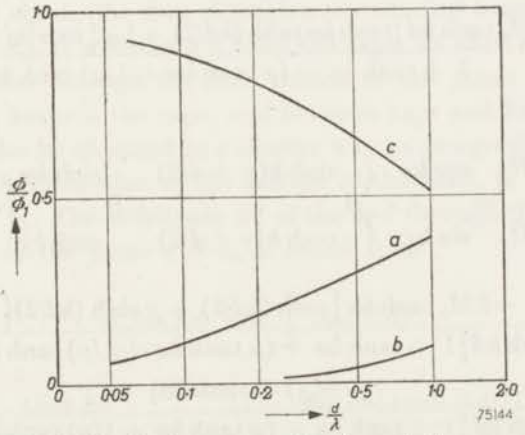

Fig. 26. Fraction of the flux in the tape passing through the space U (fig. 22) beneath the tape (*a*), through the space S between tape and head (*b*), and through the head H (*c*), as a function of d/λ.

From the approximation (8c) it is seen that, since Φ_0 is proportional to the tape thickness d, the flux Φ in the head is independent of tape thickness if the wavelength λ is comparable to d. This was observed

already by Kornei [28]) and Herr, Murphy and Wetzel [29]). The reasons why only a surface layer contributes to the reproduced flux are twofold. On the one hand the demagnetizing field increases for deeper layers so that for a tape in contact with the head, the flux is decreased everywhere except on the contacting side, as is illustrated in fig. 22*b*; and on the other hand the deeper layers do not contribute to the flux in the head because of the rapid decrease of the reproduced flux with increasing distance.

Another question is that the recorded magnetization will decrease with the distance from the recording head, while here the recorded magnetization was supposed to be constant over the depth of the tape.

3. Perpendicular magnetization

In the case of perpendicular magnetization the recorded magnetization may be written as

$$M_{0x} = 0, \quad M_{0y} = M_0 \sin kx,$$

and therefore eq. (4) becomes

$$\Delta H_x = 0, \quad \Delta H_y = 0.$$

The solution is obtained along the same lines as in the case of longitudinal magnetization in the preceding section. With the same boundary conditions it is found that

for $-\infty < y < -d$:

$$\begin{matrix}\mu_0 H_x \\ \mu_0 H_y\end{matrix} = \begin{matrix}\cos kx \\ \sin kx\end{matrix} \times \frac{M_0 \tanh kd \{\tanh ka \tanh (kd/2) + 1/\mu\} \exp \{k(y+d)\}}{1 + \tanh ka + (\mu \tanh ka + 1/\mu) \tanh kd}; \quad (9a)$$

for $-d < y < 0$:

$$\begin{matrix}\mu\mu_0 H_x \\ \mu\mu_0 H_y\end{matrix} = \begin{matrix}\cos kx \\ \sin kx\end{matrix} \times \left\{ A \begin{matrix}\sinh k(y+d/2) \\ \cosh k(y+d/2)\end{matrix} + B \begin{matrix}\sinh ky \\ \cosh ky\end{matrix} \right\}, \quad (9b)$$

where

$$A = \frac{-2M_0 \tanh ka \{\cosh (kd/2) + \mu \sinh (kd/2)\}}{\cosh kd \{1 + \tanh ka + (\mu \tanh ka + 1/\mu) \tanh kd\}},$$

$$B = \frac{-M_0(1 - \tanh ka)}{\cosh kd \{1 + \tanh ka + (\mu \tanh ka + 1/\mu) \tanh kd\}};$$

for $0 < y < a$:

$$\begin{matrix}\mu_0 H_x \\ \mu_0 H_y\end{matrix} = \begin{matrix}-\cos kx \sinh k(a-y) \\ +\sin kx \cosh k(a-y)\end{matrix} \times \frac{M_0 \tanh kd \{1/\mu + \tanh (kd/2)\}}{\cosh ka \{1 + \tanh ka + (\mu \tanh ka + 1/\mu) \tanh kd\}}. \quad (9c)$$

If the wavelength is large compared with the thickness of the tape ($kd \ll 1$) then in first approximation

$$\mu_0 H_y \approx -\frac{M_0}{\mu}\left(1 - \frac{1}{1+\tanh ka}\,\frac{kd}{\mu}\right)\sin kx\,. \qquad (10)$$

Thus if a demagnetization factor is defined as $D = -\mu_0 H_y / M_y$ then it follows from eq. (10), in combination with $M_y = M_0 \sin kx + (\mu - 1)\mu_0 H_y$, that to a first approximation

$$D = 1 - kd\,\frac{1}{1+\tanh ka}\,.$$

The demagnetization factor is unity for long wavelengths, independent of the question whether the tape is in contact with the head or not. This is easily seen in the case of a tape magnetized homogeneously in the perpendicular direction. For then, if $\mathrm{div}\boldsymbol{B} = \mathrm{div}(\boldsymbol{M} + \mu_0 \boldsymbol{H}) = 0$ is applied to a surface element of the tape it appears that $\mu_0 H_y = -M_y$, thus $D = 1$. It is further seen that in this case $M_y = M_0/\mu$. The magnetization has decreased by a factor μ under the influence of the demagnetizing field, and it is consequently to be expected that at low frequencies the output decreases at the same rate.

If the wavelength is not long compared with the thickness of the tape, then the field as well as the magnetization are functions of the depth in the tape. To obtain the flux through a reproducing head, with its gap in the plane $x = x_0$, at a distance a from the tape, we shall again calculate separately the flux through the cross section of this plane with the tape, the flux closing beneath the tape, and between tape and head. As before, the result can also be obtained in a shorter way by integrating the vertical component of the induction at the surface of the head, in this case from $x = \lambda/4$ to $x = x_0$. The amplitude Φ_1^1 of the flux through the cross section bd of the tape in the plane $x = x_0$ is found from

$$\Phi_1^1 \cos kx_0 = b \int_{-d}^{0} \mu\mu_0 H_x \mathrm{d}y\,,$$

which gives

$$\Phi_1^1 = \Phi_0 \frac{\tanh kd}{kd}\,\frac{(1 - \mathrm{than}\, ka)\tanh(kd/2)}{1 + \tanh ka + (\mu \tanh ka + 1/\mu)\tanh kd}\,.$$

For a free tape ($a = \infty$, and hence $\tanh ka = 1$) it is seen that $\Phi_1^1 = 0$, thus there is no resultant longitudinal flux component. The configuration of the magnetization in the tape is sketched in fig. 27*a*. The longitudinal components of the magnetization in the upper and the lower half of the tape are of opposite direction and cancel each other out owing to

symmetry. If now the tape is brought in the vicinity of a reproducing head the symmetry is disturbed (fig.27*b*), the longitudinal induction in the lower part of the tape being greater than in the upper part. Thus a residual longitudinal flux results.

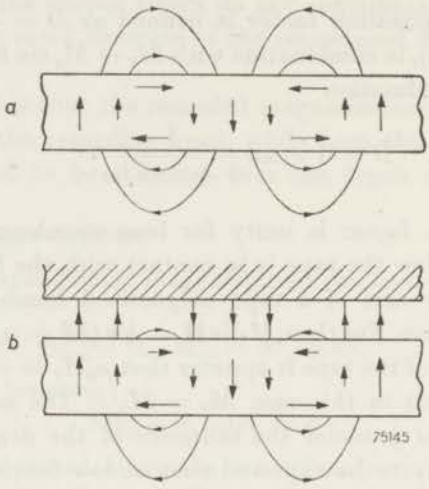

Fig. 27. Schematic illustration of the magnetization in the tape for perpendicular magnetization

a. free tape,
b. tape approached from one side by a reproduction head.

The amplitude of the flux closing beneath the tape is

$$\Phi_2^1 = \Phi_0 \frac{\tanh kd}{kd} \frac{\tanh ka \tanh (kd/2) + 1/\mu,}{1 + \tanh ka + (\mu \tanh ka + 1/\mu)\tanh kd},$$

and of the flux closing between tape and head.

$$\Phi_3^1 = \Phi_0 \frac{\tanh kd}{kd} \frac{\{1/\mu + \tanh (kd/2)\} (1 - 1/\cosh ka)}{1 + \tanh ka + (\mu \tanh ka\, 1/\mu) \tanh kd}.$$

It is seen from the formulae (9), and from fig.27*b*, that the flux beneath the tape has the same direction as the residual flux in the tape; therefore the amplitude of the flux variations in the head, and thus in the coil, is $\Phi_p = \Phi_1^1 + \Phi_2^1 - \Phi_3^1$. Hence

$$\Phi_p = \Phi_0 \frac{\tanh kd}{kd} \frac{1/\mu + \tanh (kd/2)}{1 + \tanh ka + (\mu \tanh ka + 1/\mu) \tanh kd} \frac{1}{\cosh ka}. \quad (11)$$

The recorded magnetization being a sine and the reproduced flux a

cosine function there is a 90° phase difference between the two. In the case of the longitudinal magnetization no phase shift occurred.

In fig.28*a* the values of Φ_p/Φ_0 computed from eq.(11) are plotted against d/λ for a constant ratio $a/d = \frac{1}{4}$ and several values of the permeability. In fig.28*b* these curves are drawn for a constant value $\mu = 4$ of the permeability and some values of the parameter a/d.

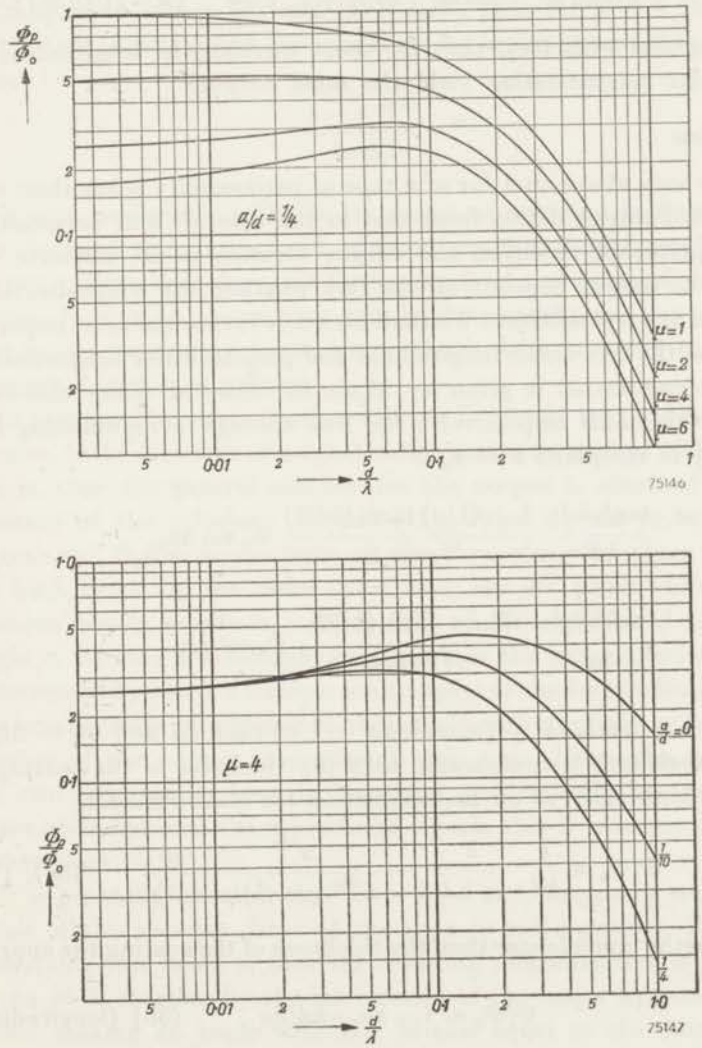

Fig. 28. Reproduced flux as a function of wavelength in the case of perpendicular magnetization.

a. for some values of the permeability, and $a/d = \frac{1}{4}$,

b. „ „ „ „ „ space between head and tape, and $\mu = 4$.

For small values of ka and kd the first approximation of (11) gives

$$\Phi_p/\Phi_0 = (1/\mu)\{1 - ka + kd\,(\mu/2 - 1/\mu)\}. \qquad (11)$$

In effect the output is inversely proportional to the permeability as a consequence of the demagnetization.

For shorter wavelengths, $kd/2 > 1$, Φ_p/Φ_0 is approximately equal to

$$\Phi_p/\Phi_0 \approx kd\,\frac{1}{1+\mu\tanh ka}\;\frac{1}{\cosh ka} = \frac{1}{kd}\,\frac{2}{\mu+1}\;\frac{e^{-2ka}}{1-e^{-2ka}\,(\mu-1)/(\mu+1)}. \qquad (11c)$$

This is identical with (8c), thus for short wavelengths longitudinal and perpendicular magnetization yield the same output.

4. Discussion

We have seen above that for of a tape of permeability other than unity the calculated output differs from that in the case of unit permeability, while the permeability enters the output formula in an intricate way. Moreover the output depends on the fact whether the magnetization is longitudinal or perpendicular. We shall here first review the most important formulae for the two cases, longitudinal and perpendicular magnetization.

If the magnetization is given by $M_0 \sin kx$, directed along the x-axis and along the y-axis respectively, the flux through a reproducing head with its gap in the plane $x = x_0$ is

$$\frac{\tanh kd}{kd}\;\frac{1 + (1/\mu)\tanh (kd/2)}{N\cosh ka}\,\Phi_0 \sin kx_0, \qquad (8)$$

and

$$\frac{\tanh kd}{kd}\;\frac{1/\mu + \tanh (kd/2)}{N\cosh ka}\,\Phi_0 \cos kx_0 \qquad (11)$$

repsectively,

where $N = 1 + \tanh ka + (\mu \tanh ka + 1/\mu)\tanh kd$ and $\Phi_0 = M_0 bd$.

If the wavelength is comparable with the thickness of the coating we may use in both cases as an approximation for these formulae

$$\Phi/\Phi_0 \approx \frac{1}{kd}\;\frac{2}{\mu+1}\;\frac{e^{-ka}}{1-e^{-2ka}\,(\mu-1)/\mu+1)}. \qquad (8c),\ (11c)$$

For wavelengths much longer than the thickness of the coating the approximations

$$\Phi/\Phi_0 \approx 1 - ka - kd/2\mu \qquad (8b)\ \text{(longitudinal)}$$

and

$$\Phi_p/\Phi_0 \approx (1/\mu)\{1 - ka + kd\,(\mu/2 - 1/\mu)\} \qquad (11b)\ \text{(perpendicular)}$$

may be used.

In this approximation the demagnetizing field is given by

$$\mu_0 H_x = -kd \frac{\tanh ka}{1+\tanh ka} M_0 \sin kx \tag{6}$$

and

$$\mu_0 H_y = -\frac{1}{\mu}\left(1-\frac{kd}{\mu}\frac{1}{1-\tanh ka}\right) M_0 \sin kx \tag{10}$$

respectively.

Comparison of eqs (8) and (11) shows that for $\mu = 1$ the amplitude factors are identical and can moreover be brought into the more simple form

$$\frac{1-e^{-2\pi d/\lambda}}{2\pi d/\lambda} e^{-2\pi a/\lambda}. \tag{8a}$$

This is in conformity with the statement of section 4 in Part II where it was deduced that for a head of finite gap length the amplitude of the output variations is the same for longitudinal and perpendicular magnetization. It may be shown that this holds generally for any type of head that is symmetrical with respect to the y-plane provided that the field-strength vanishes at infinity.

In practice the magnetization will not be purely longitudinal or perpendicular. If the direction of magnetization makes an angle α with the positive x-axis, then the general solution for the output is obtained by a superposition of the solutions (8) and (11), where Φ_0 has to be replaced by $\Phi_0 \cos\alpha$ and $\Phi_0 \sin\alpha$ respectively. At short wavelengths, where the solutions for both cases are the same apart from the 90° phase shift, the superposition merely results in a phase shift of the reproduced signal over an angle α. At long wavelengths the output of the perpendicular component is decreased by about a factor μ with respect to the longitudinal component. For small values of α therefore the superposition merely results in the reduction of the output proportional with $\cos\alpha$. Since the amplitudes of the two components have to be added quadratically because of the 90° phase shift between the reproduced signals this is true even for angles α rather close to 90°.

It is generally believed that for a good high-frequency response a high value of the coercive force of the tape is indispensable. The reasoning underlying this belief is that the resulting magnetization is reprensented in the M-H diagram by the intersection of the major hysteresis loop with a line making an angle with the M-axis equal to the demagnetization factor; so that, especially at the higher frequencies where the demagnetization is great, the output will increase with the coercive force.

In reality, however, the recorded magnetization has to be such that

the major loop is never reached; for this would mean that the peaks of a recorded sine wave are cut off, which would result in a distortion of the signal. It is therefore obvious that in the formulae (8) and (11) the coercive force does not appear.

The real influence of the coercive force on the reproduction of the high frequencies has to be seen as follows. Firstly there is a general but not very strict relation between coercive force and permeability of magnetic materials, in the sense that a low coercive force is accompanied by a high permeability, and vice versa [30]). Since a high permeability reduces the high-frequency output this may also roughly be said of a low coercive force.

Secondly, a low coercive force in principle limits the level at which a good frequency response can be obtained without distortion at the high frequencies. But even in the case of the low coercive tape ($\mu_0 H_c = 75 \cdot 10^{-4}$ Vsec/m^2) used in our experiments other sources of distortion come into play before this level is reached.

V. COMPARISON WITH EXPERIMENTS

1. Experimental arrangement

Having discussed in the preceding parts the macroscopic behaviour of the magnetic tape in a homogeneous field, the influence of the gap on recording and reproduction, and the magnetic behaviour of a sinusoïdally magnetized tape under the influence of the demagnetizing field, we shall now compare the results of these calculations with the observed relation between input and output voltage.

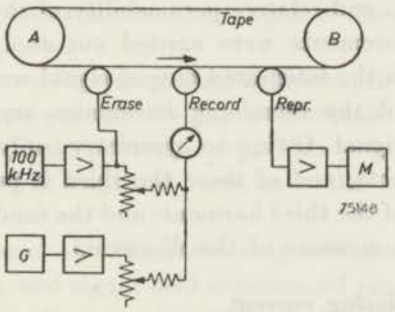

Fig.29. Schematic diagram of experimental arrangement.

A schematic diagram of the arrangement used in the experiments is given in fig. 29. An endless loop of tape is transported with constant speed in the indicated direction over the rollers A and B. Thus an element of the tape has to pass successively the erasing, the recording and the reproducing head.

The erasing head is fed by a 100 kHz oscillator and amplifier which delivers a current of sufficient strength to remove any previous recording. From the same generator is derived the biasing current for the recording head. The amplitude of this current may be adjusted with a potentiometer.

A low-frequency generator G supplies an input current of variable amplitude and frequency which is, after suitable amplification, superposed on the biasing current through the recording head. The frequency range covered extends from 50 Hz to 15000 Hz.

The variations of the flux through the coil of the reproducing head due to the passage of the magnetized tape induce in this coil a voltage that is amplified and fed to a voltmeter, a distortion meter, or other mea-

suring device *M*. For some of the measurements it is useful to insert an integrating network in the amplifier. In this way the rise with frequency of the output voltage is compensated and the resulting voltage is a better measure of the flux in the tape.

Both recording and reproducing head consist of a magnetic circuit with a gap 0·4 mm high, filled with a 6 μm non-magnetic and non-conducting distance piece. The actual gap length, measured under a microscope, varies from 6·5 to 8 μm. The cross-section of the rest of the circuit is such that its reluctance is negligible compared with that of the gap. The core is built up of mu-metal laminations, the thickness of which are 50 μm for the recording and 100 μm for the reproducing head. The number of turns of the coil is 125 for the recording and 350 for the reproducing head.

The tape used for the present experiments was the same as that with which the magnetic measurements of section 3 of Part III were carried out. The width of the tape was $b = 6{\cdot}3$ mm, thickness of the magnetic coating $d = 15$ μm, and relative permeability of the tape $\mu = 3{\cdot}6$.

Distortion measurements were carried out at a frequency of 250 Hz. The fundamental in the integrated output signal was cut off by a 400 Hz high-pass filter and the remaining harmonics amplified and compared with the original signal. Owing to symmetry, only odd harmonics occur in tape measurements, and of these the third is predominant. The ratio of the amplitudes of the third harmonic and the fundamental in the output signal is used as a measure of the distortion.

2. Output versus biasing current

If the biasing current is varied, at a constant signal current of 250 Hz an output curve is obtained (fig. 30) with a maximum at a biasing current of 3 mA. At low frequencies, where the recorded wavelength is long

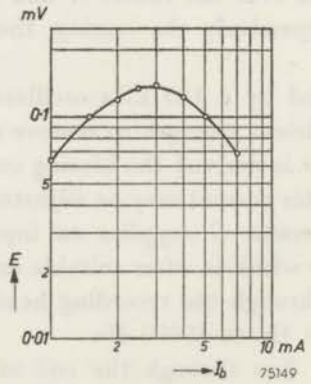

Fig.30. Output voltage as a function of biasing current, at a signal current of 0·2 mA, 250 Hz.

compared with the length of the gap of the reproducing head and with the thickness of the tape it can be assumed that the recorded flux is reproduced without error. For instance at the frequency of 250 Hz and a tape speed of 0·76 m/sec the wavelength is 3 mm. It may be seen in fig. 23*b* that for a tape thickness of 15 μm the influence of the demagnetization in the tape is very small. The gap loss at this frequency is completely negligible. Moreover, at this frequency it can be assumed that the phase of the signal is constant during the time an element of tape passes that region where the recording process takes place.

It should therefore be possible to obtain the variation of the recorded flux with the biasing current from the experiments and calculations of the preceding chapters. A complication here is the variation of the field with the distance at which an element of tape passes the head. The simplest way for the calculation of the flux is to suppose at first that biasing- and signal-current are varied proportionally. Then the variation of the recorded magnetization with the depth in the tape can be constructed in the following way.

From fig. 7 can be read the maximum fieldstrength H that is experienced by an element of tape passing the gap at a certain distance y, expressed in the fieldstrength H_0 deep in the gap. This gives in fig. 31*a* H/H_0 as a function of y for a gap length of 7 μm, as is the case for the recording head used.

The relation between the remanent magnetization and the maximum values of the biasing and signal field experienced can be read from fig. 18. For a signal field equaling one tenth of the biasing field this remanent magnetization is given in fig.31*c* as a function of the biasing field. For

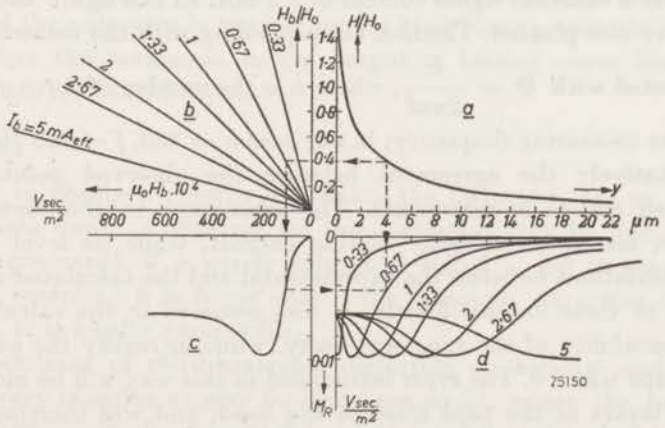

Fig.31. Construction of the recorded magnetization as a function of biasing current and distance to the head. For explanation see text.

reasons of simplicity it is here supposed that the recorded magnetization is longitudinal. The field in the gap is found from $H_0 = nI/l$, where n is the number of turns of the recording coil, I the current through this coil, and l the gap length. Therefore, the biasing field H_b is derived from

$$\mu_0 H_b = \frac{H_b}{H_0} \frac{\mu_0 n I_b}{l},$$

where I_b is the biasing current. Hence the remanent magnetization as a function of y is found by combining figs 31*a* and 31*c* with fig.31*b*, the latter giving $\mu_0 H_b$ as a function of Hb/H_0 for some values of the biasing current. This construction gives the curves of fig.31*d* for different values of the biasing current. The remanent flux in a tape is obtained by integration of M_R over the surface of the tape.

It is seen that for small biasing currents the recorded magnetization has a maximum near the side of the tape nearest the recording head, and therefore the total flux depends to a large amount on the distance between tape and head. For larger values the maximum is shifted to deeper layers of the tape.

In order to obtain the remanent flux as a function of the biasing current for a constant value of the signal current it must be remembered that in fig.31*d* the signal current increases proportionally to the biasing current. Since the signal current is supposed to be very small the recorded magnetization may be taken as proportional to the signal current, which enables us to reduce the curves to one signal-current level.

Carrying out the computation for a tape of 15 μm thickness and 6·2 mm width, and for some values of the space between head and tape, the curves of fig.32 are found for the variation of the recorded flux with the biasing current at a constant signal current of 0·2 mA. In this figure the measured points are also plotted. The flux corresponding with the measured voltage is computed with $\Phi = \frac{E}{2\pi n f}$, where n is the number of turns of the head, and f the measuring frequency; in our case $n = 350$, $f = 250$ Hz.

Qualitatively the agreement between the observed points and the calculated curves is reasonable. The maximum in the measurements, however, occurs at a higher biasing current, while its level is lower.

The deviations between the experimental and the calculated curve may be due to three causes. Firstly, it was assumed in the calculation that the permeability of the tape was unity, while in reality the permeability of the tape was 3·6. The error introduced in this way will be most marked for the layers of the tape close to the head, and will therefore be most pronounced at small currents, where these layers give the main contribution to the recorded flux. Secondly, the direction of the recorded magnetiza-

tion varies over the thickness of the tape and is, moreover, dependent on the amplitude of the biasing current. Thirdly, the direction of the biasing field varies as the tape passes the gap, this variation being especially rapid for the layers of the tape close to the head. It is therefore to be expected that an output reduction will occur at small biasing currents.

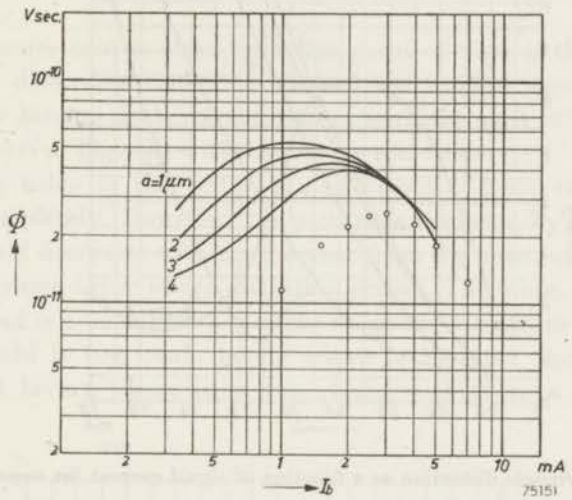

Fig.32. Computed (full curves) and measured flux (circles) as a function of biasing current.

From fig.31*d* it is seen that the decrease of the recorded flux for large values of the biasing current is due mainly to the finite thickness of the magnetic coating of the tape, so that the top of the curve shifts to values of y beyond the coating. It is therefore understandable that for homogeneous tapes the reduction in the output for high biasing currents is slower and therefore the maximum in the output *vs* biasing curve less is pronounced than for coated tapes.

3. Distortion

In order to obtain a good reproduction the distortion has to be kept within certain limits. A measure for this distortion may be found in the harmonics generated, if a purely sinusoïdal signal is fed to the system. For sound recording it is found that if the harmonic distortion does not exceed 2% it is hardly perceptible.

The dependence of third-harmonic distortion on biasing- and signal-current is very complex as may be seen from fig.33, where the ratio (d_3) of third harmonic to fundamental is plotted against the signal current for different values of the biasing current. We shall not attempt here to give a full explanation of the peculiarities of these distortion curves.

However, some features may be explained starting from the measured M-H curves of fig.18.

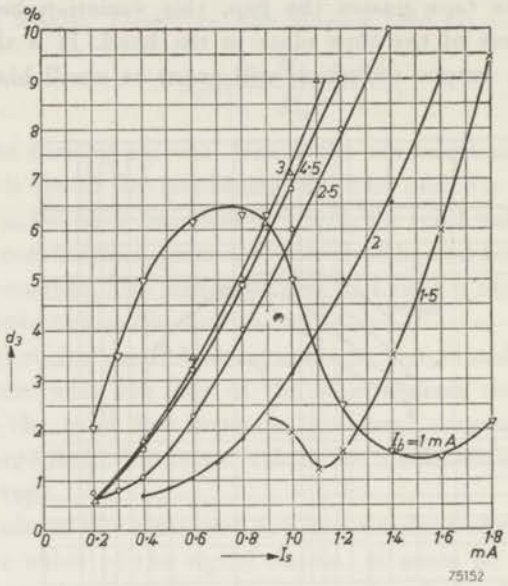

Fig.33. Third harmonic distortion as a function of signal current for some values of the biasing current.

For small values of the a.c. field (smaller than the coercive force) these curves are convex in the origin, then follow a linear part and next, owing to saturation effects, they become concave with respect to the H-axis. Thus in first approximation they may be described by

$$M = aH + bH^3 - cH^5.$$

The inflexion point of this curve is situated at

$$H = \sqrt{\frac{3}{10}\,\frac{b}{c}}.$$

If now H varies with time according to $H = H_0 \sin\omega t$, it follows that

$$M = (a + \frac{3}{4} b\, H_0^2 - \frac{5}{8} c\, H_0^4) H_0 \sin\omega t - (\tfrac{1}{4} b - \frac{5}{16} c\, H_0^2)\, H_0^3 \sin 3\omega t -$$

$$- \frac{1}{16} c\, H_0^5 \sin 5\omega t$$

Hence we see that the third harmonic is zero for $H_0 = \sqrt{4b/5c}$, which means that the r.m.s. value of the signal field equals approximately the fieldstrength of the inflexion point.

From fig.18 it is seen that for small biasing fields the inflexion point is found at signal fields of approximately $\mu_0 H \approx 10^{-2}$ Vsec/m². Since for small biasing fields a magnetization is recorded close to the head only (cf. fig.31*d*), i.e. where the field is about 4/10 of that in the gap, the minimum of the third harmonic is to be expected in this case for signal currents of approximately 1·4 mA. This is in good agreement with the measured values.

Another feature that is clear from this point of view is that the minimum in the distortion curves is reached for smaller signal fields the higher are the biasing fields, in accordance with the shift to smaller fields of the *M-H* curves (fig. 18) with increasing a.c. fields.

For biasing fields of the order of the coercive force the minimum disappears completely. However, the picture is confused by the fact that the biasing field decreases with the distance from the head, whence there is always a transition layer where distortion occurs. Therefore, the resulting flux in the head is a superposition of the magnetization from layers where the biasing field is too weak, layers where it has just the appropriate strength, and layers where it is too strong and gives a reduction in the output.

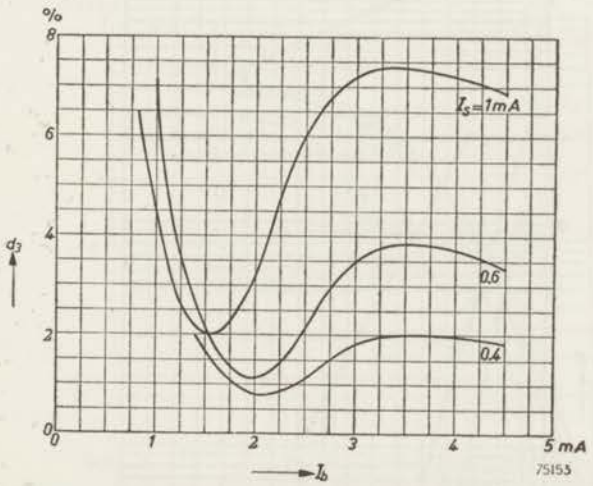

Fig.34. Third harmonic distortion as a function of biasing current, for some values of the signal current.

Usually the distortion is plotted against the biasing field for constant values of the signal field. These curves (fig.34) can be constructed from fig.33. From what was said above it is clear that the minima of these curves may be partly due to the extinction of a third harmonic generated in the surface layers by a third harmonic of opposite sign generated deeper in the tape. If now the signal frequency is raised and the recorded wave-

length consequently decreased, the demagnetizing effect has more influence on the inner than on the surface layers and thereby the cancelling of the third harmonic is disturbed. This explains why it is sometimes observed that, when at low frequencies the distortion has been brought within reasonable limits by a critical choice of the biasing current, there may still be an appreciable distortion for higher signal frequencies.

4. Frequency characteristic

In the preceding chapters we discussed the output at low frequencies, where the demagnetization and gap loss could be neglected. When the frequency is raised we can assume that the recorded magnetization is at first independent of frequency, i.e. as long as there is no appreciable phase change of the signal field during the passage of an element of the tape past the gap.

The loss due to the finite length of the reproducing gap for a tape of unit permeability can be found from fig.9. For a gap of 7 μm as used in the experiments this gives, even at the shortest wavelength used (13 μm occurring at a tape speed of 19 cm/sec and a frequency of 15 kHz) a

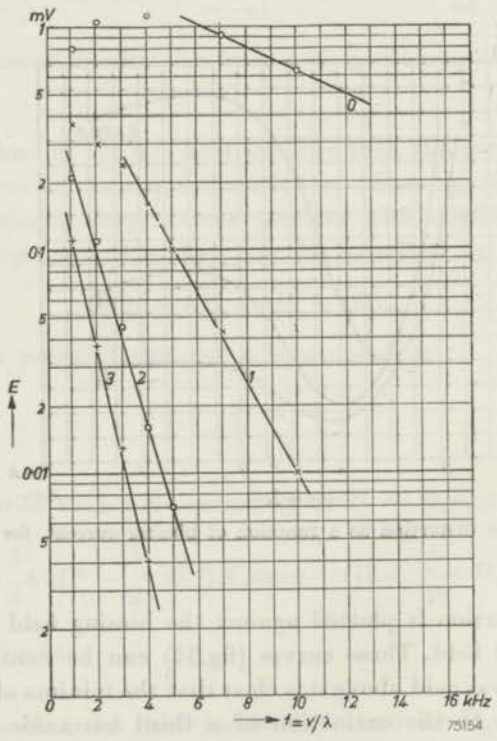

Fig.35. Voltage measured across reproducing coil as a function of frequency with 0, 1, 2 or 3 paper sheets between head and tape.

deviation not exceeding 6 dB. It may be assumed therefore that the application of the correction according to fig.9 will not introduce serious errors in our case where $\mu \approx 4$.

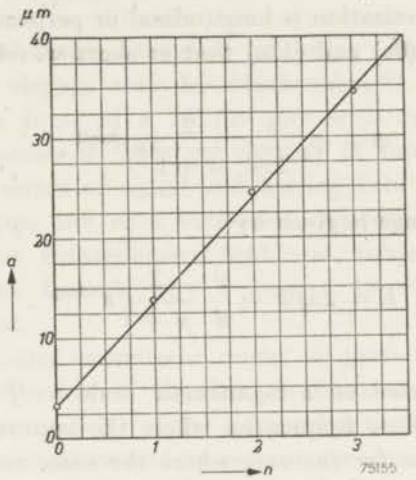

Fig.36. Calculated separation between tape and head against the number of sheets between the two.

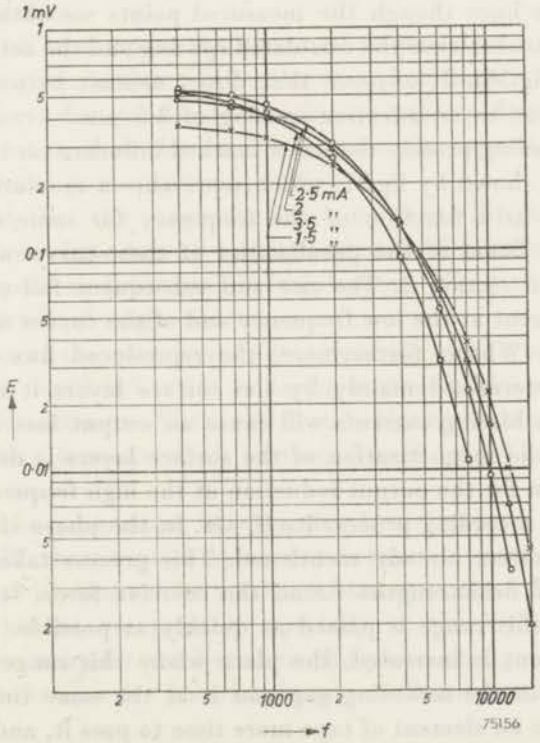

Fig.37. Frequency response for some values of the biasing current.

The reason for the output reduction that remains after this correction has been applied is to be sought mainly in the combined effect of demagnetization and distance to the head as given by eqs(8) and (11) depending on whether the magnetization is longitudinal or perpendicular.

It is seen from eqs(8c) and (11c) that at short wavelength the reproduced flux is

$$\Phi = \Phi_0 \frac{\lambda}{2\pi d} \frac{2}{\mu + 1} e^{-2\pi a/\lambda},$$

while the output voltage is given by

$$E = 2\pi f \Phi = \frac{v}{d} \frac{2}{\mu + 1} e^{-2\pi a/\lambda}.$$

If therefore E is plotted on a logarithmic scale vs $f = v/\lambda$ a straight line is obtained for those frequencies where the approximation holds.

In fig.35 this is done for the case where the same recording is played back with one or more thin sheets of paper (9 μm each) placed between tape and reproducing head. By computing a in the above equations from the slopes of the lines though the measured points we obtained a satisfactory agreement between the calculated spacing and the actual thickness of the sheets (fig.36). It appears that direct contact between head and tape is equivalent to an effective spacing of 3·5 μm.

That the recording process too has a marked influence on the frequency characteristic is shown by fig.37, which represents a measurement of the reproduced flux as a function of the frequency for some values of the biasing current. Some of the peculiarities of these curves are clear from the discussion in section 2. The rise and subsequent fall of the output with biasing current at the low frequency end of the curves was explained in that section. Where, furthermore, the reproduced flux at the high frequencies is determined mainly by the surface layers it is clear from fig.31*d* that high biasing currents will cause an output loss at these frequencies, since the magnetization of the surface layers is decreased.

Another reason for the output reduction at the high frequency end may be found in the recording process itself, viz. in the phase change during the recording process already mentioned. This process takes place in a critical range of fieldstrengths round the coercive force. It is therefore important that this range is passed as quickly as possible. If, however, the biasing current is increased, the place where this range is passed is shifted away from the recording gap and is at the same time extended. It will then take an element of tape more time to pass it, and in this way a loss at high frequencies is caused due to the phase change.

Since the change of phase is proportional to the frequency f, and as the time of passing the critical range is inversely proportional to the tape speed v, the determining factor for the loss is the recorded wavelength $\lambda = v/f$.

This effect, which may be called recording demagnetization, was determined in an elegant way by Muckenhirn [31]). He measured the field distribution in front of a 20 μm gap with an 8 μm wire, then caclulated the sequence of fields an element of tape was subjected to by the combined action of signal and biasing field during the passage of the recording gap, and next measured the remanent magnetization when a tape in a homogeneous field was subjected to the same sequence of changes. In this way a loss of 19 dB was found at a wavelength of 25 μm.

In our case a similar experiment might be performed making use of the computed distribution of the field in front of the recording gap. Because of the inhomogeneity of the field owing to the small gap length, however, these computations and measurements would be rather delicate and tedious. It may be estimated that for the smaller gap used in our case the output reduction will be less than in the case of the 20 μm gap used by Muckenhirn.

If now we wish to compare the measured frequency characteristic with the calculations given in Part IV for the case that there is no loss in the recording, we have first to decide whether to use eq.(8) or eq.(11) and we have to insert in these formulae values for the tape thickness d, the spacing a, and the permeability μ.

It is believed that the magnetization, though its direction may vary over the thickness of the tape, is mainly longitudinal because the maximal value the magnetizing field value is longitudinal. We shall therefore use eq.(8) for longitudinal magnetization.

The thickness of the magnetized layer depends on the biasing current. It is seen from fig.31*d* that for a biasing current of 1·5 mA $d = 8$ μm is a reasonable estimate. With a 2·5 mA biasing current, practically the whole coating is magnetized, so that $d = 15$ μm. The permeability may be taken as $\mu = 4$.

Taking for the separation between head and tape $a = 2$ μm it is seen from fig.38 that a good agreement between experimental and the theoretical curve is obtained for a 1·5 mA biasing current. For the 2·5 mA curve the deviations are greater, especially at the higher frequencies. These deviations may be attributed to the phase change during the recording, which has, as we have seen, more influence at higher biasing currents.

In conclusion we may state that the theoretical considerations of

Parts II, III and IV are sufficient to account for the essential features in the recording process determined experimentally.

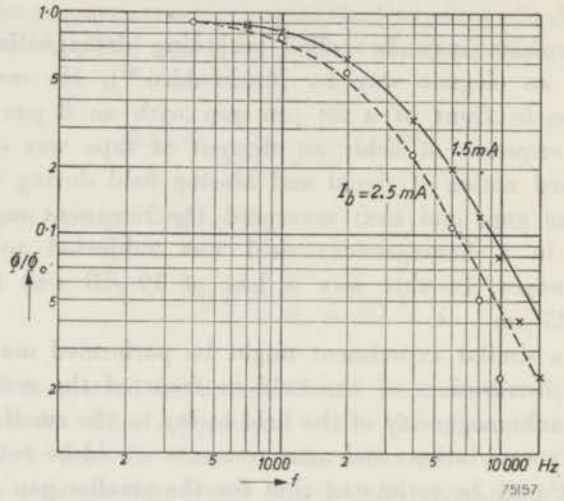

Fig.38. Calculated and measured frequency response for two values of the biasing current.

In order to obtain an exact quantitative agreement it would be necessary to make more detailed calculations which, however, would require an extremely accurate determination of the geometric configuration and of the magnetic properties of the special tape considered. In our opinion, however, such a very laborious extension of the theory would not reveal any essentially new aspects of the problem. Also the technical value would be extremely limited.

VI. CHANGE IN THE RECORDING WITH TIME

1. Conservation of a magnetic recording

In the preceding parts we have discussed the processes that lead to the recording of information consisting of the variation of a quantity with time as the variation of the magnetic state along the length of a magnetic tape, and the subsequent reproduction whereby the original information is regained as a variation with time. In this part we shall see if the information stored on the tape can be preserved over a period without being subjected to unacceptable changes.

One kind of change that a recording can undergo is that it is attenuated proportionally to the recorded magnetization. For the recording of sound a certain amount of such a proportional attentuation can be tolerated since a decrease of 10% of the amplitude of a reproduced signal can hardly be heard and a greater decrease can be compensated afterwards by suitable amplification. Even if the higher frequencies should be attentuated more than the lower ones this could be overcome by the use of correcting networks. These corrrections, however, are limited by the background noise since this, too, is amplified.

More serious in the case of sound recording is, that extraneous fields may introduce magnetizations that are incoherent with the recorded magnetization. Even if these additional magnetizations are at a very low level they may be very annoying.

These additional magnetizations may be introduced when a tape is stored on a reel, because then the magnetization in one layer of the tape may give rise to a stray magnetization in adjacent layers of the reel. The magnetization effected in a this way is called spurious or accidental printing, or print-effect. It may happen that this spurious magnetization extends over several layers on the reel, to the inside as well as to the outside. In playback this is heard as one or more pre- and post-echoes. The former, in particular, may be very disturbing in sound recording.

Of course care should be taken that a recorded reel is not subjected to a field of some strength, for then a partial erasing may take place. Here the accompanying print effect will be far more serious since this field will act as a biasing field superimposed on the field from the adjacent layers.

In the next section we shall investigate, experimentally as well as theore-

tically, the change of magnetization with time under the influence of weak fields.

2. Print effect

Investigations into the print effect have been carried out by Lippert [32]), Vinzelberg [33]), Johnson [34]), Daniel and Axon [35]) and Wendt [36]). From these investigations it appears that the magnitude of the print effect depends on a number of factors, inter alia, the wavelength of the recorded magnetization, the distance between the layers, the temperature, the time during which the tapes have been in contact and the time elapsed since the ending of the contact. In this section we shall give the observed dependence of the print effect on some of these factors, while in the next section we shall discuss the relation with the magnetic after-effect.

The printing was obtained by bringing part of a loop of a virgin tape for a prescribed time into contact with a magnetized tape in an U-shaped groove made in a piece of metal. In order to rule out as many irreproducible effects as possible, the contact pressure was kept constant, and the temperature of the metal could be controlled. The loop was then played back in a loop-testing machine. Only sinusoïdal signals were used for the measurements.

The amplitude of the printed flux as a function of the amplitude of the magnetizing flux is given in fig.39. Here the flux is plotted on a logarithmic scale along both axes. The slope of the straight line obtained in this way

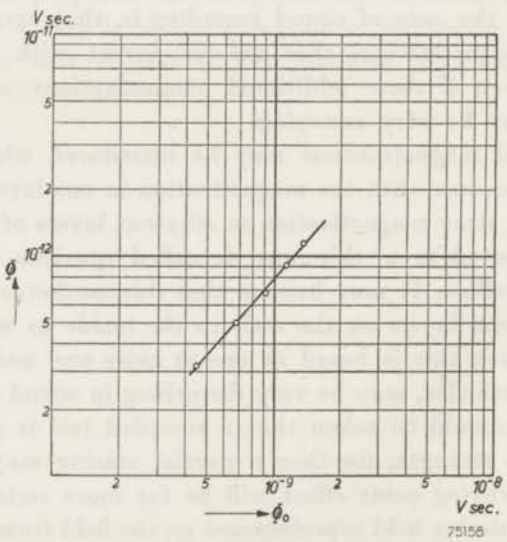

Fig. 39. Amplitude of the printed flux as a function of the amplitude of the flux in the printing tape.

is 1·1, showing that the printed flux is practically proportional to the printing field.

Fig.40 gives the variation of the printed flux Φ with the wavelength λ. Along the abscis is plotted $v/\lambda = f$, where v is the tape velocity at play back and f the corresponding frequency. It is seen that the printed flux has a maximum at a frequency of 2000 Hz for the tape speed of 762 mm/sec used. This corresponds with a wavelength of 380 μm.

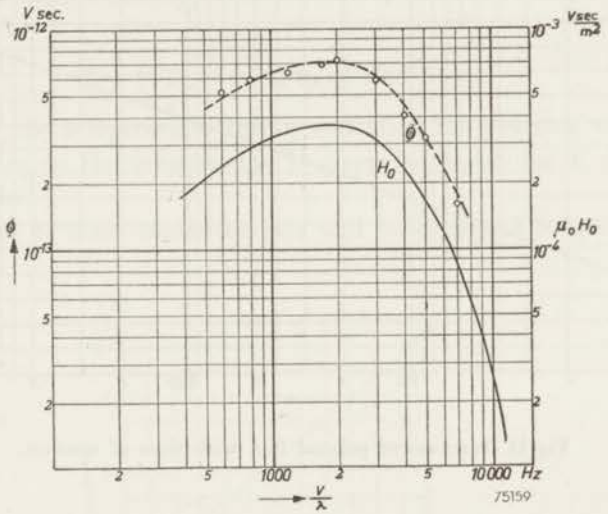

Fig.40. Dependence of printed flux Φ and printing field H_0 on wavelength.

This may be understood in the following way. The field at a distance y from a longitudinally magnetized tape is given by eq.(5c) of Part IV. In this equation we can take $a = \infty$, since no highly permeable metal is present. In first approximation ($\pi d/\lambda \ll 1$) this equation gives for the absolute value of the field.

$$\mu_0 H = B_0 \frac{\pi d}{\lambda} e^{-2\pi y/\lambda}.$$

This shows the general behaviour of the field as a function of the wavelength. At long wavelengths it increases proportionally with $1/\lambda$ because the apparent magnetic poles in the tape increase proportionally with $1/\lambda$. At short wavelengths it decreases exponentially with $1/\lambda$ because of the decrease of the field with the distance from the tape. The maximum value of the field is obtained for $\lambda = 2\pi y$.

If two tapes are brought into contact as is done for the measurement of the print effect we can calculate the amplitude of the printing field with formula (5c) of Part IV, if it is assumed that the permeability of

the receiving tape does not affect the field. For a tape with a total thickness $\Delta = 56$ μm and a coating $d = 16$ μm, of permeability $\mu = 1{\cdot}7$, as used in the experiments and for an amplitude of the recorded flux $\Phi_0 = 0{\cdot}9.10^{-9}$ Vsec this yields the full drawn curve of fig.40, representing the printing field H_0 as a function of frequency. The dashed curve of this figure is a shift of the field curve. The close agreement with the measured points

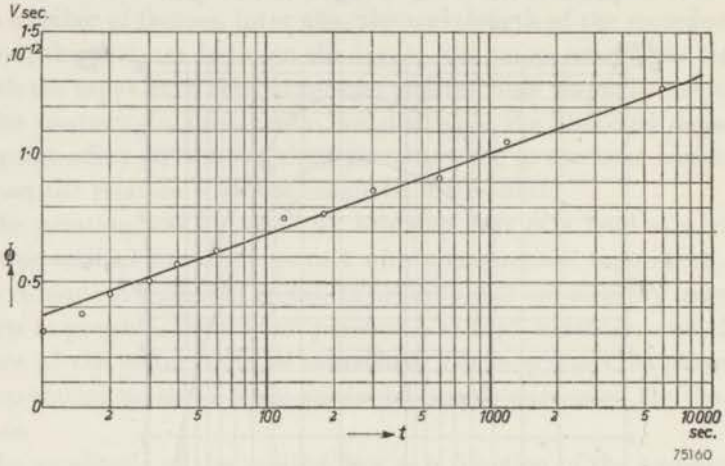

Fig.41. Increase of printed flux with time of contact.

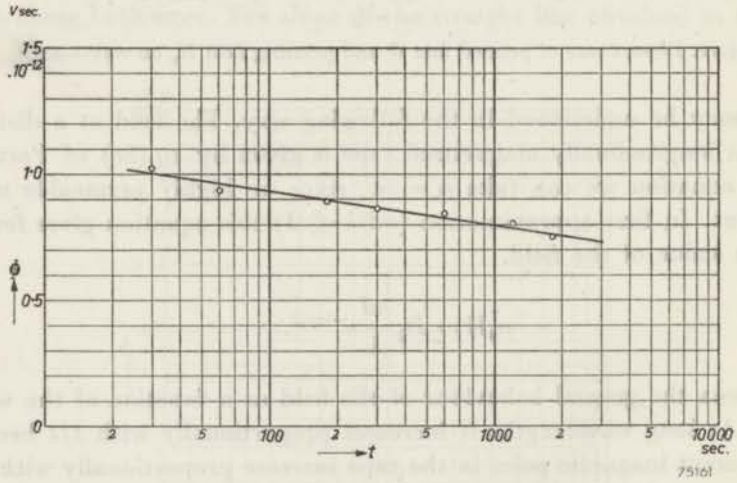

Fig.42. Decrease of printed flux with time after the ending of contact.

shows once more the proportionallity of the printed flux with the magnetizing field.

The change of the printed flux with time is shown in figs 41 and 42. In the first it is plotted against the time t_1 during which the tapes have

been in contact, measured at a constant time $t_2 = 1$ min after the ending of the contact. If the flux is plotted on a linear and the time on a logarithmic scale a straight line is obtained obeying the equation

$$\Phi = 0{\cdot}14.10^{-12} \ln t_1 \text{ Vsec.}$$

Fig. 42 shows the change in the printed flux with the time t_2 since the ending of the contact between the tapes, after a contacting time $t_1 = 10$ min. Here again, an approximately linear relation is obtained, given in this instance by

$$\Phi = (1{\cdot}21 - 0{\cdot}061 \ln t_2).10^{-12} \text{ Vsec.}$$

In both cases the temperature during and after the printing was 30 °C. The dependence on the temperature is given by fig.43, for $t_1 = 10$ min and $t_2 = 1$ min.

The outcome of these measurements will be discussed below.

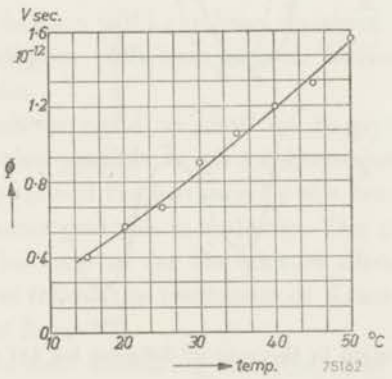

Fig.43. Variation of printed flux with temperature.

3. Magnetic lag

If the fieldstrength in a magnetizable medium is changed suddenly, part of the magnetization will, in general, not follow instantaneously but with a certain time lag. A consequence of this lag is that energy losses will occur in an alternating field.

From the measurements made by Preisach [37]) it appears that a difference has to be made between a lag for which the principle of superposition does, and a lag for which it does not hold. Néel [38]) distinguishes the two as "trainage reversible" and "trainage irreversible". The first is found for only a limited number of substances in a limited range of temperatures, and the magnetization reaches a definite limit. Snoek [39]) has found

that the reason for this lag has to be sought in are location of carbon and nitrogen atoms in the crystal lattice.

The second type of lag is found with all ferromagnetic materials. Here the magnetization does not reach a limit but keeps on increasing with ln*t*. Already Preisach mentions as a possible explanation the influence of the Brownian motion on delayed Barkhausen jumps. This idea has been worked out more in detail by Street and Woolley [40]) and by Néel [41])[42]).

Physically, the difference between diffusion lag and fluctuation lag may be seen as follows. The moment after a change of the magnetic field, the Bloch wall between two domains reaches a position of minimal potential energy (*A* in fig. 44). In the case of diffusion lag the strain in the wall will induce some atoms to take other positions in the lattice. In this way the potential minimum is displaced somewhat, e.g. to *B* in fig. 44*a*. If

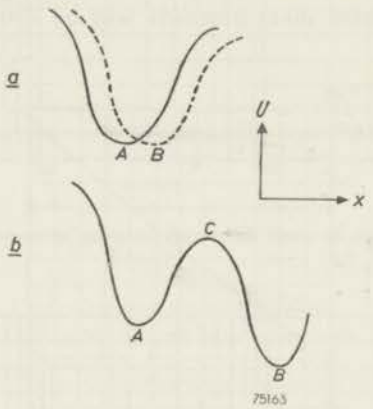

Fig.44. Potential distribution in the case of diffusion lag (*a*) and fluctuation lag (*b*).

the field is removed the potential hole will after a certain time regain its original position. In the case of fluctuation lag the minimum at *A* is separated by a potential barrier at *C* from a deeper minimum at *B* (fig.44*b*). By exchange with the lattice the energy of the wall will fluctuate and at a certain time be sufficient to cause the wall to cross the potential barrier.

From the measurements in the preceding section it is seen that the print effect does not approach a certain limit, and we will therefore assume that the print effect can be ascribed to the fluctuation lag.

The physical picture we can form is as follows. In a magnetic particle the wall separating two domains of different direction of magnetization has a number of preferred positions separated from each other by potential barriers. By interaction with the lattice the wall will occasionally have sufficient energy to cross a potential barrier. In this way an equilibrium position will finally be attained if a large number of walls is present.

However, for a position separated by a high potential barrier from a position with lower energy the chance of crossing will be very small, though the latter position has the highest probability. The attainment of the equilibrium state can be accelerated by a rise in temperature, which gives the wall more energy to cross the potential barrier, or by the superposition of an a.c. field as is the case in the ideal magnetization. In this case the height of the potential barrier oscillates so that at a constant energy of the wall the chance of escape is increased.

If now a direct field is applied, the potential energy of the wall is increased proportionally to its displacement. The result is that a redistribution of the walls over the potential holes will take place as a kind of diffusion process. This redistribution is accompanied by an increase of the magnetization in the direction of the applied field. In this picture the permeability must be seen as a reversible displacement of the walls in the potential holes, effecting an increase of the mean magnetic moment in the direction of the field. If after a certain time the field is removed a permanent magnetization will have been obtained that will be attenuated again by an analogous diffusion process, having as a final result the original distribution.

With this picture in mind we shall try to give an explanation of the print effect. It is also possible to give a discussion for the case where the magnetization is obtained for instance by the rotation of the magnetization of single the same particles in a cluster. The mathematical treatment will be seen for this case as for the picture discussed here.

We shall here first follow the treatment of Kramers [43]) of the Brownian motion in a field of force.

Le x be the coordinate describing the location of the Bloch wall between two domains, and $U(x)$ the potential of the wall. The equation of motion is

$$m\ddot{x} + r\dot{x} = K(x) + X(t)\,,$$

where m is the apparent mass of the wall, r the damping, $K(x) = -\partial U/\partial x$, and $X(t)$ a term describing the influence of the fluctuations. The existence of the apparent mass of a Bloch wall is due to the moment of inertia of the spins that rotate while a wall is displaced. The magnitude of this mass was calculated by Döring [44]) and Becker [45]).

In the case where the damping r is such that K does not change appreciably over a distance $\sqrt{mkT/r}$, Kramers deduces the equation of diffusion.

$$\frac{\partial \sigma}{\partial t} = -\frac{\partial}{\partial x}\left(\frac{K\sigma}{r} - \frac{kT}{r}\frac{\partial \sigma}{\partial x}\right),$$

where $\sigma(x, t)\mathrm{d}x$ is the fraction of an ensemble of equal walls that has at a time t a coordinate between x and $x + \mathrm{d}x$.

In the stationary case this gives a diffusion current

$$w = \frac{K\sigma}{r} - \frac{kT}{r}\frac{\partial\sigma}{\partial x} = -\frac{kT}{r}e^{-U/kT}\frac{\partial}{\partial x}(\sigma e^{-U/kT}).$$

Let us now consider a potential function as illustrated in fig.45. Since

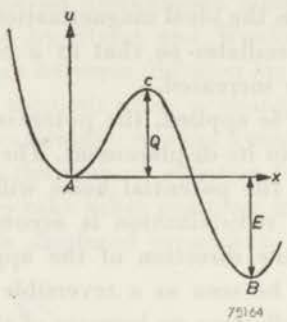

Fig.45. Considered potential distribution.

the diffusion current w is constant between A and B, integration of the equation

$$we^{U,kT} = -\frac{kT}{r}\frac{\partial}{\partial x}(\sigma e^{U/kT})$$

between these points gives.

$$\int_A^B e^{U/kT}\,dx = \frac{kT}{r}\sigma e^{U/kT}\Big|_A^B$$

Let the potential at A be represented by $U = \alpha x^2$, and at C by $U = Q - \beta(x-x_A)^2$. Then the integral is found from

$$\int_A^B e^{U/kT}\,dx \approx \int_{-\infty}^{+\infty} e^{Q-(\beta x-x_0)^2/kT}\,dx = \sqrt{\frac{kT}{\beta}}\,e^{Q/kT},$$

and in the case that Q is high enough for a Boltzmann partition to be established, the number of walls in the potential hole at A is found from

$$n_A \approx \int_{-\infty}^{+\infty} \sigma_A e^{-\alpha x^2/kT}\,dx = \sqrt{\frac{kT}{\alpha}}\,\sigma_A.$$

If there are no walls at B, $\sigma e^{U/kT}\Big|_B^A = \sigma_A$, and the number of walls escaping in unit time from A to B is given by

$$W_{AB} = \frac{1}{\tau}e^{-Q/kT}n_A, \text{ where } \tau = \frac{r}{\sqrt{\alpha\beta}}.$$

We shall extend this result of Kramers to the case that walls are also present in the potential hole B. This gives a diffusion current from B to A which must be substracted from the current from A to B. If the potential hole at B has the same shape as that at A, viz. $U = E + \alpha(x-x_B)^2$, then the diffusion current from B and A is given by

$$w_{BA} = \frac{1}{\tau} e^{-(Q+E)/kT} n_B.$$

Let N be the total number of walls divided over A and B then

$$\frac{dn_A}{dt} = w_{BA} - w_{AB} = \frac{1}{\tau} \left\{ e^{-(Q+E)/kT} (N-n_A) - e^{-Q/kT} n_A \right\}.$$

This is satisfied by

$$n_A = \frac{N\varepsilon}{1+\varepsilon} + \left(n_0 - \frac{N\varepsilon}{1+\varepsilon}\right) e^{-(1+\varepsilon)q t/\tau},$$

where

$$\varepsilon = e^{-E/kT},$$
$$q = e^{-Q/kT}.$$

If a magnetic field H is applied, E as well as Q will be changed. Let $2\Delta I$ be the increase of the magnetization in the direction of H when a wall jumps from A to B, then the decrease of the energy at x is given by

$$\Delta U = \frac{2\Delta I}{x_B - x_A} Hx.$$

Hence the potential difference between A and B is now $E + 2H\Delta I$, and, if C is midway between A and B the potential difference between C and A is $Q - H\Delta I$.

Had an equilibrium been established before the field was applied, $n_{A0} = N\varepsilon/(1+\varepsilon)$, then at a time t_1 after the application of the field, the number of walls in A would be given by

$$n_{A1} = \frac{N\varepsilon}{e^{2h}+\varepsilon} \left\{ 1 + \left(\frac{e^{2h}+\varepsilon}{1+\varepsilon} - 1\right) e^{-(1+\varepsilon e^{-2h})\, q e^h t_1/\tau} \right\},$$

where $h = \dfrac{H\Delta I}{kT}$.

If at that moment the field is removed the distribution a time t_2 later will be given by

$$n_{A2} = \frac{N\varepsilon}{1+\varepsilon} + \left(n_{A1} - \frac{N\varepsilon}{1+\varepsilon}\right) e^{-(1+\varepsilon)\, q t_2/\tau}.$$

The increase of the magnetization is

$$2\,\Delta I(n_{A0}-n_{A2}) =$$
$$= 2\Delta I\,N\varepsilon\left(\frac{1}{1+\varepsilon}-\frac{1}{e^{2h}+\varepsilon}\right)\left(1-e^{-(1+\varepsilon e^{-2h})qe^{h}t_1/\tau}\right)\,e^{-(1+\varepsilon)qt_2/\tau}.$$

In reality not all the potential holes will have the same energy difference E, nor all the potential barriers the height Q. Therefore a summation has to be carried out over all E's and Q's. It may be assumed that in the region considered all values of E are of equal probability. When $n(Q)\mathrm{d}E\mathrm{d}Q$ denotes the number of holes with a potential difference between E and $E+\mathrm{d}E$ and a potential barrier between Q and $Q+\mathrm{d}Q$, integration over E gives

$$\mathrm{d}I = 2kT\,\Delta I\,n(Q)\,\mathrm{d}Q\int_0^\infty\left(\frac{1}{1+\varepsilon}-\frac{1}{e^{2h}+\varepsilon}\right)\left(1-e^{-(1+\varepsilon e^{-2h})qe^{h}t_1/\tau}\right)e^{-(1+\varepsilon)qt_2/\tau}\,\mathrm{d}\varepsilon.$$

For small values of h the main contribution comes from small values of ε. Hence, neglecting in first approximation ε in the exponent it is found that

$$\mathrm{d}I \approx 4\,kT\,\Delta I\,h\,n(Q)\,\mathrm{d}Q\left\{e^{-qt_2/\tau}-e^{-q(e^{h}t_1+t_2)/\tau}\right\}.$$

Integration over Q gives integrals of the type

$$\int_0^\infty n\,(Q)\;e^{-ce^{-Q/kT}}\,\mathrm{d}Q.$$

The function $e^{-e^{-x}}$ is zero for $x\ll 0$, unity for $x\gg 0$, and goes from 0 to 1 in a small interval round $x=0$. If therefore $f(x)$ is a function that changes little in this interval then

$$\int_0^\infty f(x)e^{-e^{-x+\alpha}}\,\mathrm{d}x \approx \int_\alpha^\infty f(x)\,\mathrm{d}x.$$

Hence

$$I \approx 4(\Delta I)^2\int_{kT\ln t_2/\tau}^{kT\ln(e^{h}t_1+t_2)/\tau} n(Q)\,\mathrm{d}Q. \qquad (1)$$

4. Discussion

The formula deduced above gives the magnetization at a time t_2 after the removal of a field H that has been applied during a time t_1 to an assembly of demagnetized particles. This is exactly what is done in the experiments on the print effect.

The formula shows that the printed magnetization I is proportional

to the applied printing field H and to the hatched area in fig.46, representing $n(Q)$ as a function of Q.

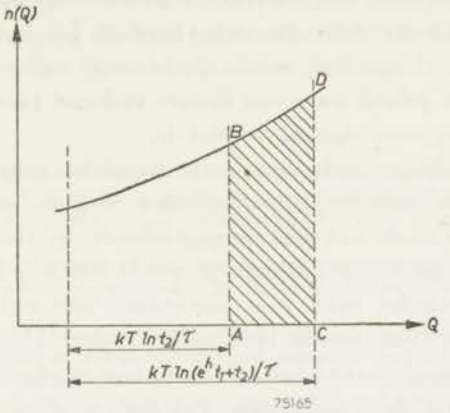

Fig.46. Fictitious distribution of the number of potential-barriers over Q. The hatched area shows those barriers that contribute to the print effect.

The physical interpretation is that for the particles to the left of AB the potential barrier is so low and therefore the time of escape so small that these particles have first crossed the barrier under the influence of the printing field, but have returned already during the time t_2. On the other hand the potential barrier for the particles to the right of CD is so high that the printing time t_1 was not sufficient to effect an appreciable crossing. In the derivation it is assumed that the limits AB and CD are sharp while in reality there is a small region of transition.

It is seen that in the course of time the limit AB is displaced proportional to $kT\ln t_2$ while, if $e^h t_1 > t_2$, the limit CD is displaced proportionally to $kT\ln t_1$. This explains qualitatively the experimental relation between the print, and t_2 and t_1 respectively. Néel arrives at the same result but along a different line.

That the experimental proportionality constant is higher for the increase with $\ln t_1$ than for the decrease with $\ln t_2$ may be explained if $n(Q)$ increases with Q. This could explain also the rapid increase of the printed magnetization with the temperature.

A certain increase of $n(Q)$ with Q is to be expected. For in the ideal case all the potential barriers should be of equal height Q_0, where Q_0 is such that the barrier is just crossed instantaneously if the coercive field-strength is applied. The function $n(Q)$ is in that case a peak function with a peak at Q_0. In reality the Q's have a certain distribution round Q_0 which means that $n(Q)$ will rise for small Q, fall for high Q, and have a maximum that is reached for field of about coercive strength. For the small printing fields of about $4 \cdot 10^{-4}$ sec/m^2 we can therefore expect to be in a rising part of the $n(Q)$ versus Q curve.

Samenvatting

In dit proefschrift worden enkele problemen van physische en mathematische aard behandeld, die zich voordoen bij de magnetische registratie op band, en wel speciaal enkele problemen welke zich voordoen bij de registratie van geluid waar een lineair verband tussen het oorspronkelijke en het weergegeven signaal vereist is.

In de inleiding wordt een kort overzicht gegeven van het principe en sommige technische bijzonderheden van de magnetische registratiemethode, en van de ontwikkelingsgeschiedenis. De onderlinge samenhang van de te behandelen problemen wordt uiteengezet.

Het magnetische veld voor de spleet van enkele eenvoudige typen van opneemkoppen wordt berekend in deel II als oplossing van een tweedimensionaal potentiaalprobleem. Uitgaande van de berekende veldverdeling wordt door toepassing van het reciprociteitstheorema berekend welk deel van de magnetische strooiflux van een band, waarop een bekende magnetisatie is vastgelegd, door de spoel van een weergeefkop gaat. Aangetoond wordt dat de bekende formule voor de spleet verliezen $\sin(\pi l/\lambda)/(\pi l/\lambda)$ alleen geldt voor een hypothetisch geval, en een meer algemene formule wordt afgeleid.

De methoden van opnemen die tot een lineair verband voeren tussen de vastgelegde magnetisatie en het inkomende signaal worden beschouwd in deel III. Bijzondere aandacht wordt besteed aan de methode van het hoogfrequente bijveld en de samenhang die bestaat tussen deze methode en die van de ideale magnetisatie. Deze discussie wordt gebaseerd op metingen in homogene velden. Een magnetisch model wordt gegeven waarmee de lineariserende werking van het h.f. bijveld kan worden verklaard.

In deel IV wordt het magnetische veld in en om een sinusvormig gemagnetiseerde band berekend. De gevallen van longitudinale en van loodrechte magnetisatie worden afzonderlijk behandeld. Indien de permeabiliteit van de band groter is dan 1, heeft het ontmagnetiserende veld een vermindering van de teweeg gebrachte magnetisatie tot gevolg. Alleen voor het geval dat de permeabiliteit van de band 1 is hebben longitudinale en loodrechte magnetisatie dezelfde flux in de kop tot gevolg.

In deel V worden de berekeningen van de voorafgaande delen vergeleken met de experimenten. Vooral het verband tussen output en bijstroom, de vervorming als functie van de signaal- en bijstroom, en de output als functie van de frequentie worden bekeken.

Tenslotte wordt in deel VI de verandering bestudeerd van een magnetische registratie met de tijd, in het bijzonder de magnetisatie die tot stand komt onder invloed van zwakke magnetische velden afkomstig van

naburige lagen van een opgewikkelde band en die bekend staat onder de naam echo-effect. Er worden metingen van het echo-effect gegeven en vergeleken met berekeningen van de magnetische nawerking die gebaseerd zijn op de Brownse beweging in een potentiaalveld. De logarithmische toename van de echo met de tijd wordt hiermee verklaard.

Summary

In this thesis some problems are treated concerning the physics and mathematics of magnetic recording. In particular those problems are dealt with that arise in the recording of sound, where a strictly linear relationship between original and reproduced signal is required.

The introduction gives a brief survey of the principle, of some technical details, and of the history of the magnetic recording method. The mutual relation of the problems to be treated is explained.

The magnetic field in front of the gap of some simple types of recording head is calculated in Part II as the solution of a two-dimensional potential problem. Applying the reciprocity principle the magnetic flux through the coil of a reproducing head, originating from a sinusoïdally magnetized tape in front of the gap, is deduced from this field distribution. It is shown that the well-known gap-loss formula $\sin(\pi l/\lambda)/(\pi l/\lambda)$ only holds in a theoretical case, and a more general formula is given.

The recording methods leading to a linear relationship between the recorded magnetization and the input signal are discussed in Part III. Special attention is paid to the a.c. biasing method and its relation to the method of ideal magnetization. This discussion is based on magnetic measurements in homogeneous fields. A magnetic model explaining the linearizing action of the a.c. biasing field is discussed.

Part IV contains the calculation of the magnetic field that exists in and around a sinusoïdally magnetized tape, the cases of longitudinal and perpendicular magnetization being treated separately. When the permeability of the tape is greater than unity, the demagnetizing field in the tape effects a decrease of the reproduced magnetization. The flux in an ideal reproducing head is calculated for this case. It is shown that longitudinal and perpendicular magnetization produce the same flux in the head only when the permeability of the tape is 1.

In Part V a comparison is given between values derived from the formulae derived in the preceding parts and the experimental data. The relation between output and biasing current, the distortion as a function of signal- and biasing-current, and the output as a function of frequency are given special consideration.

Finally in Part VI changes of a magnetic recording with time are discussed; in particular the magnetization by weak magnetic fields from adjacent layers of tape. Measurements of this so called print effect are compared with the magnetic lag calculated from the Brownian movement of particles in a field of force. The logarithmic increase of the print effect with time is explained in this way.

Résumé

Dans cette thèse on discute quelques problèmes concernant les bases théoriques et mathématiques de l'enregistrement sur ruban magnétique. Spécialement sont traités les problèmes qui se présentent dans l'enregistrement du son, où une relation strictement lineaire est exigée.

Dans l'introduction on rappelle succinctement les principes et quelques détails techniques de la méthode d'enregistrement sur ruban magnétique et de son histoire. La relation entre les problèmes à discuter est exposée.

Le champ magnétique devant l'entrefer de quelques types de têtes d'enregistrement est calculé dans la partie II, comme solution d'un problème de potentiel à deux dimensions. Utilisant la distribution du champ ainsi calculée on calcule le flux magnétique parcourant la bobine d'une tête de reproduction, provenant d'un ruban sur laquelle une magnétisation quelconque est enregistrée. On démontre que la formule bien connue pour les pertes par entrefer, $\sin(\pi l/\lambda)/(\pi l/\lambda)$, est seulement valable dans un cas théorique, et une formule plus générale est donnée.

Les méthodes d'enregistrement conduisant à une relation plus linéaire entre la magnéti-

sation enregistrée et le signal d'entrée sont discutées dans la partie III, en particulier la méthode de la magnétisation à polarisation h.f. et la relation qui existe entre cette méthode et celle de la magnétisation idéale. Cette discussion est basée sur des mesures dans des champs homogènes. Une théorie magnétique qui explique l'action de linéarisation de ce champ de polarisation est donnée.

Dans la partie IV on calcule le champ magnétique existant dans un ruban magnétisé suivant une sinusoïde et celui autour de ce ruban. Les cas de magnétisation longitudinale et perpendiculaire sont traités séparément. Le champ de démagnétisation dans le ruban produit une diminution de la magnétisation rémanente seulement dans le cas où la perméabilité du ruban est superieure à l'unité. Pour ce cas le flux dans une tête de reproduction idéale est déterminé. C'est seulement dans le cas d'une perméabilité égale à 1 que les magnétisations longitudinale et perpendiculaire produisent le même flux dans la tête.

Dans la partie V on compare le résultat des calculs des parties précédentes aux expériences. Sont considérées en particulier la relation entre la tension de sortie et le courant de polarisation, entre la distorsion et le courant du signal et de polarisation, et entre la tension de sortie en fonction de la fréquence.

Pour finir on discute dans la partie VI le changement d'un enrégistrement magnétique avec le temps, spécialement la magnétisation acquise sous l'influence des champs magnétiques provenant de rubans avoisinants, connue comme effet d'écho. Des mesures de cet effet sont mentionnées et comparées à des calculs sur le traînage magnétique. Ces calculs sont basés sur le mouvement Brownien des particules dans un champ de force. L'incrément logarithmique de l'effet d'écho est expliqué de cette façon.

Zusammenfassung

In dieser Dissertation werden einige Probleme physikalischer und mathematischer Art behandelt, welche mit der Aufzeichnung auf magnetisierbarem Band zusammenhängen, und zwar insbesondere einige Probleme, welche bei der Schallaufzeichnung auftreten, bei der eine lineare Beziehung zwischen dem ursprünglichen und dem reproduzierten Signal erforderlich ist.

In der Einleitung wird eine kurze Übersicht des Prinzips und einiger technischer Einzelheiten der magnetischen Schallaufzeichnungsmethode sowie deren Geschichte gegeben. Die Beziehung der behandelten Probleme zueinander wird erläutert.

Teil II enthält die Berechnung des Magnetfeldes vor dem Spalt eines Aufnahmekopfes als Lösung eines zweidimensionalen Potentialproblems. Mit Hilfe dieser berechneten Feldverteilung und dem Reziprozitätstheorem wird der von einem Band mit bekannter Magnetisierung herrührende Magnetfluss durch die Spule eines Wiedergabekopfes berechnet. Es wird gezeicht, dass die bekannte Spaltfunktion $\sin(\pi l/\lambda)/\pi l/\lambda)$ nur in einem hypothetischen Falle gültig ist. Eine allgemeinere Formel wird abgeleitet.

Im Teil III werden die Aufnahmemethoden diskutiert, welche zu einer besser linearen Beziehung zwischen aufgezeichneter Magnetisierung und Eingangssignal führen. Insbesondere wird die Hochfrequenz-Vormagnetisierung besprochen und die Beziehung dieser Magnetisierungsmethode und derjenigen der idealen Magnetisierung. Dieser Diskussion sind magnetische Messungen in homogenen Feldern zugrunde gelegt. Ein Modell der magnetischen Vorgänge, mit denen die linearisierende Wirkung des Hochfrequenzfeldes erklärt werden kann, wird erläutert.

Teil IV enthält die Berechnung des Magnetfeldes innerhalb und ausserhalb eines sinusförmig magnetisierten Bandes. Longitudinale und senkrechte Magnetisierung werden einzeln behandelt. Ist die Permeabilität des Bandes grösser als 1, so hat das entmagnetisierende Feld einen Rückgang der remanenten Magnetisierung zur Folge. Der Fluss in einem idealen Wiedergabekopf wird für diesen Fall berechnet. Es zeigt sich, dass nur im Falle einer Permeabilität des Bandes gleich 1 die longitudinale und senkrechte Magnetisierung denselben Fluss im Kopf erregen.

Im Teil V werden die Berechnungen der vorigen Teile mit den Versuchen verglichen. Insbesondere die Beziehung zwischen Ausgangsspannung und Vormagnetisierungsstrom, zwischen nichtlinearer Verzerrung und Eingangs- und Vormagnetisierungsstrom, und zwischen Ausgangsspannung und Frequenz werden erörtert.

Schliesslich wird im Teil VI die Änderung einer Aufzeichnung als Funktion der Zeit besprochen, insbesondere die Magnetisierung unter Einfluss schwacher, von benachbarten Bändern herrührenden magnetischer Felder, der sogenannte Kopiereffekt. Die Ergebnisse von Messungen dieses Kopiereffektes werden aufgeführt und mit den Resultaten von Berechnungen der magnetischen Nachwirkung verglichen, welche den Brownschen Bewegungen in einem Kraftfelde zugrunde gelegt sind. Die logarithmische Zunahme des Kopiereffektes in Abhängigkeit von der Zeit wird auf diese Weise erklärt.

REFERENCES

[1]) E. Schüller, Elektrotech. Z. **56**, 1219-1221, 1935.
[2]) S. J. Begun, Magnetic Recording, Murray Hill Books, New York, 1949.
[3]) V. Poulsen, Ann. Phys., Lpz. **3**, 754-760, 1900.
[4]) C. Stille, Elektrotech. Z. **51**, 449-451, 1930.
[5]) F. Pfleumer, German patent No. 500900, 31 Jan. 1928.
[6]) V. Poulsen and P. O. Pederson, U. S. Patent 873084, 10 Dec. 1907.
[7]) W. L. Carlson and G. W. Carpenter, U. S. Patent 1640881, 30 Aug. 1927.
[8]) K. Nagai, S. Sasaki, J. Endo, Nippon elect. Commun. Engng 445-447, Nov. 1938.
[9]) Akust. Z. **6**, 264, 1941.
[10]) H. Lübeck, Akust. Z. **2**, 273-295, 1937.
[11]) R. Herr, B. F. Murphy and W. W. Wetzel, J. Soc. Mot. Pict. Engrs **52**, 77-87, 1949.
[12]) R. L. Wallace, Bell Syst. tech. J. **30**, 1145-1173, 1951.
[13]) A. D. Booth, Brit, J. appl. Phys. **3**, 307-308, 1952.
[14]) D. L. Clark and L. L. Merrill, Proc. Inst. Radio Engrs. N.Y. **35**, 1575-1579, 1947.
[15]) G. N. Watson, A treatise on the theory of Bessel functions. Cambridge Univ. Press 1922, p. 180.
[16]) Ibid t VIII, p. 752.
[17]) S. J. Begun, Audio Engng **32**, 11-13, 39, Dec. 1948.
[18]) P. E. Axon, B.B.C. Quart. **5**, 46-53, 1950.
[19]) O. Schmidbauer, Frequenz **6**, 319-324, 1952.
[20]) A. H. Mankin, Trans. Inst. Radio Engrs PGED-1, 16-21, 1952.
[21]) M. Camras, U. S. Patent 2351004, 13 June 1944.
[22]) H. Toomin and D. Wildfeuer, Proc. Inst. Radio Engrs N. Y. **32**, 664-668, 1944.
[23]) L. C. Holmes and D. L. Clark, Electronics **18**, 126-136, July 1945.
[24]) W. Steinhaus and E. Gumlich, Verh. dtsch phys. Ges.
[25]) C. Kittel, Phys. Rev. **73**, 801-811, 1948.
[26]) R. M. Bozorth, Ferromagnetism, v. Nostrand Company, New York 1951, p. 486.
[27]) L. Neel, C. R. Acad. Sci. Paris **224**, 1488-1490, 1947.
[28]) O. Kornei, Electronics **20**[2], 124-128, Aug. 1947.
[29]) R. Herr, B. F. Murphy and W. W. Wetzel, J. Soc. Mot. Pict. Engrs **52**, 77-87, 1949.
[30]) C. Kittel, Rev. mod. Phys. **21**, 541-583, 1949.
[31]) O. W. Muckenhirn, Proc. Inst. Radio Engrs, N.Y., **39**, 891-897, 1951.
[32]) W. Lippert, Elektrotechnik, Berl. **1**, 56-62, 1947.
[33]) B. Vinzelberg, Funk u. Ton **2**, 633-639, 1948.
[34]) S. W. Johnson, J. Soc. Mot. Pict. Engrs **52**, 619-627, 1949.
[35]) E. D. Daniel and P. E. Axon, B. B. C. Quart. **5**, 241-256, 1950.
[36]) B. Wendt, Veröff. ZentLab. Anilin. photogr, Abt. VII, 314-329, 1951.
[37]) F. Preisach, Z. Phys. **94**, 277-302, 1935.
[38]) L. Neel, J. Phys. Radium **12**, 339-351, 1951.
[39]) J. L. Snoek, Physica, 's-Grav. **6**, 161-170, 1939.
[40]) R. Street and J. C. Woolley, Proc. phys. Soc. Lond. A **62**, 562-572, 1949.
[41]) L. Néel, Ann. Géophys. **5**, 99-136, 1949.
[42]) L. Néel, J. Phys. Radium **11**, 49-61, 1950.
[43]) H. A. Kramers, Physica, 's-Grav. **7**, 284-304, 1940.
[44]) W. Döring, Z. Naturf. **3a**, 373-379, 1948.
[45]) R. Becker, J. Phys. Radium **12**, 332-338, 1951.

STELLINGEN

I.

Terwijl men moet verwachten, dat in het algemeen de formules voor de spleetcorrectie wijzigingen zullen moeten ondergaan ten gevolge van de permeabiliteit van de band, kan men bewijzen dat dit voor een band tussen 2 vlakke polen waarvoor de formule $\sin(\pi l/\lambda)/(\pi l/\lambda)$ geldt (sectie II 2 van dit proefschrift) niet nodig is.

II.

Op p.53 wordt een demagnetisatiefactor gedefinieerd voor het geval dat hogere machten van kd dan de eerste worden verwaarloosd. Het heeft echter ook nog zin van een demagnetisatiefactor te spreken wanneer grootheden van de orde k^2d^2 in aanmerking worden genomen.

III.

Het patroon der krachtlijnen aan een vrije kant van een sinusvormig gemagnetiseerde band is zodanig dat de krachtlijnen door verschuiving loodrecht op de band in elkaar overgaan.

IV.

Bij de veldcalibratie voor magnetometermetingen kan met voordeel gebruik worden gemaakt van berekeningen voor de veldverdeling.

V.

Streng gesproken zijn de eigentrillingen in een dempende ruimte niet orthogonaal. Hiermee wordt door Morse geen rekening gehouden.

P. M. Morse, Vibration and Sound, New York 1948, p. 415.

VI.

Ten onrechte verwaarlozen Keonjian en Schaffner de correlatie tussen de ruisbronnen in emitter- en collectorketen in hun berekening van de bronweerstand, die de laagste ruisfactor geeft bij *pnp*-transistors.

E. Keonjian en J. S. Schaffner, Electronics, Febr. 1953, p. 104.

VII.

Dat bij *pnp*- of *npn*-transistors de ruisfactor practisch dezelfde is bij schakeling met geaarde emitter en schakeling met geaarde basis, is een direct gevolg van de hoge impedantie van deze transistors aan de collectorzijde.

VIII.

De vervorming bij aftasting van een lateraal gesneden gramofoonplaat is kleiner dan volgens Pierce and Hunt volgt uit de door hen gegeven vergelijking voor de "poid".

J. A. Pierce and F. V. Hunt, J. Acoust. Soc. Amer. **10**, 14, 1938.

IX.

Indien men modulatieruis noemt de extra ruis die in een weergeefsysteem optreedt indien een ander dan het nulsignaal wordt doorgegeven, kan men optische dichtheidsmodulatie met recht beschouwen als een systeem met negatieve modulatieruis.

X.

Bij aftasting van een optisch geluidsspoor wordt de versterkerruis minimum als de verhouding van de breedte van de aftastspleet tot de kortste weer te geven golflengte 0,55 is, en niet 0,37 zoals Frommer beweert.

J. C. Frommer, J. Soc. Mot. Pict. Engrs **49**, 361-363, 1947.

XI.

Vasthouden aan Fries als uitgangspunt voor de wetenschapppelijke benamingen op mycologisch gebied leidt tot steeds toenemende verwarring.

XII.

De overstromingsramp van 1 Februari 1953 levert argumenten tegen het indijken van de Brabantse Biesbos.

XIII.

Het verdient aanbeveling om lensopening en sluitertijden van fototoestellen aan te geven in een maat die evenredig is met de logarithme van de doorgelaten hoeveelheid licht.